

submitted to *The Astronomical Journal* 03 SEP 2014

The Solar Neighborhood XXXVI. The Long-Term Photometric Variability of Nearby Red Dwarfs in the *VRI* Optical Bands

Altonio D. Hosey¹, Todd J. Henry¹

RECONS Institute, Chambersburg, PA 17201

altoniohosey@gmail.com, toddhenry28@gmail.com

Wei-Chun Jao¹, Sergio B. Dieterich¹, Jennifer G. Winters¹

Department of Physics and Astronomy, Georgia State University, Atlanta, GA 30302-4106

jao@astro.gsu.edu, dieterich@astro.gsu.edu, winters@astro.gsu.edu

John C. Lurie¹

Department of Astronomy, University of Washington, Seattle, WA 98195

lurie@uw.edu

Adric R. Riedel¹

Department of Astrophysics, American Museum of Natural History, New York, NY 10034

adric.riedel@gmail.com

and

John P. Subasavage¹

United States Naval Observatory, Flagstaff, AZ, 86001

jsubasavage@nofs.navy.mil

ABSTRACT

We present an analysis of long-term photometric variability for nearby red dwarf stars at optical wavelengths. The sample consists of 264 M dwarfs south of Dec. = +30 with $V - K = 3.96\text{--}9.16$ and $M_V \approx 10\text{--}20$, corresponding to spectral types M2V–M8V, most of which are within 25 pc. The stars have been observed in the VRI filters for $\sim 4\text{--}14$ years at the CTIO/SMARTS 0.9m telescope. Of the 238 red dwarfs within 25 pc, we find that only $\sim 8\%$ are photometrically variable by at least 20 mmag ($\sim 2\%$) in the VRI bands. Only four stars have been found to vary by more than 50 mmag, including GJ 1207 at 8.6 pc that experienced a single extraordinary flare, and GJ 2006A, TWA 8A, and TWA 8B, which are all young stars beyond 25 pc linked to moving groups. We find that high variability at optical wavelengths over the long-term can in fact be used to identify young stars. Overall, however, the fluxes of most red dwarfs at optical wavelengths are steady to a few percent over the long term.

The low overall rate of photometric variability for red dwarfs is consistent with results found in previous work on similar stars on shorter timescales, with the body of work indicating that most red dwarfs are only mildly variable. As expected, we find that the degree of photometric variability is greater in the V band than in the R or I bands, but we do not find any obvious trends in variability over the long term with red dwarf luminosity or temperature. We highlight 17 stars that show long-term changes in brightness, sometimes because of flaring activity or spots, and sometimes because of stellar cycles similar to our Sun’s solar cycle. Remarkably, two targets show brightnesses that monotonically increase (G 169-029) or decrease (WT 460AB) by several percent over a decade. We also provide long-term variability measurements for seven M dwarfs within 25 pc that host exoplanets, none of which vary by more than 20 mmag. Both as a population, and for the specific red dwarfs with exoplanets observed here, photometric variability is therefore often not a concern for planetary environments, at least at the optical wavelengths where they emit much of their light.

Subject headings: stars: low mass — stars: planetary systems — stars: statistics — stars: variables — techniques: photometric

¹Visiting Astronomer, Cerro Tololo Inter-american Observatory. CTIO is operated by AURA, Inc. under contract to the National Science Foundation.

1. Introduction

Red dwarfs comprise the majority of stars in the Galaxy, accounting for roughly three-quarters of all stars in the solar neighborhood (Henry et al. 2006). As the lowest luminosity hydrogen-burning stars, red dwarfs are long-lasting, stable energy producers, making them ideal candidates for planetary environments. One aspect of red dwarfs that may prove crucial to the potential of life on any orbiting planets is the consistency in the flux provided by the stars, i.e., the stellar variability. In this paper we investigate the long-term photometric variability at optical wavelengths of a large sample of red dwarfs.

The RECONS¹ (REsearch Consortium On Nearby Stars) team has gathered photometry in the *VRI* optical bands for more than 1000 nearby red dwarfs since 1999 (Winters et al. 2011; 2014). In this paper we focus on the long-term variability of 264 red dwarfs (generally within 25 pc) for which we are determining trigonometric parallaxes and searching for low mass companions as part of our astrometry/photometry effort carried out at the CTIO/SMARTS 0.9m. These stars typically have been observed on 10–30 nights each, at ~ 5 frames/night, spread over 4–14 years. This provides a rich dataset of more than 24,000 observations for the 264 stars, or nearly 100 individual frames/star. Our goals in this paper are to determine the fraction of red dwarfs photometrically variable at optical wavelengths over long time periods, to explore the dependence of variability on their luminosities and temperatures, and to identify individual stars exhibiting long-term stellar cycles. We also briefly address the effects of variability on the fluxes received by exoplanets, given recent discoveries of both gas giant and super-terrestrial exoplanets orbiting nearby red dwarfs.

Previous efforts have examined samples of M dwarfs at optical wavelengths, often in smaller numbers or over shorter time periods. In his classic study, Weis (1994) reported photometric measurements of 43 stars over an 11 year period. Jao et al. (2011) reported the first study of variability in red subdwarfs, including 130 stars from the RECONS program discussed here, observed for ~ 3 –9 years. Koen et al. (2010) provided photometry for over 700 stars, including many M dwarfs observed at multiple epochs. Transit searches have yielded rotation periods for field K and M dwarfs via HATNet (Hartman et al. 2011) and MEarth (Irwin et al. 2011) in datasets up to a few years in length that also provide guidance on overall variability rates. Gomes da Silva et al. (2012) and Robertson et al. (2013) examined spectroscopic data for 27 stars using the NaI feature and for 93 stars using the H α feature, respectively, to reveal long-term changes. Space-based efforts using Kepler data over a few months provide results for the variability of M dwarfs in the Kepler bandpass (Ciardi et al. 2011), and investigate their flare rates and intensities (Walkowicz et al. 2011; Hawley et al.

¹www.recons.org

2014). These results and ours will be discussed in more detail in §8 to provide a portrait of the dominant stellar component of our Galaxy, the red dwarfs.

2. Sample

For this study, we focus on a sample of 264 red dwarfs south of Dec. = +30 observed at the CTIO/SMARTS 0.9m, some starting as long ago as 1999. The sample is listed in Table 1, with stars falling in the ranges of $V - K = 3.96\text{--}9.16$ and $M_V \approx 10\text{--}20$, corresponding to spectral types M2V–M8V. Known cool subdwarfs have been removed, as they have been previously discussed in detail in Jao et al. (2011). Multiple systems with separations in the range 1–3'' have been omitted because even if two sources can be seen in some images, accurate photometry for each source cannot always be determined, given variable seeing. Known multiples with separations less than 1'' are treated as single sources and noted with component letters in Table 1, e.g., AB, or ABC. Multiples separated by more than 3'' can be measured separately for photometry and are given individual entries. The names are listed in Column 1 and the letter “Y” is given in Column 2 if the target is reported to be a young star, as described in Riedel et al. (2014). After the coordinates in Columns 3 and 4, we provide the VRI magnitudes and references from our program in Columns 5–8, followed by the K_s magnitude from 2MASS and the $V - K_s$ color in Columns 9–10. In Columns 11–16, we list the filter used for the long-term astrometric observations, the photometric variability in that filter calculated using methods described in §4, and various metrics of the duration of the observations, including the first and last epochs in each data series, the time coverage, the number of nights on which observations were taken, and the total number of frames (typically ~ 5 frames per night). The final columns list the parallax values and errors for stars in our sample for which we have published parallaxes to date, and the references. To determine M_V values used to analyze the sample, the published parallaxes are used, as well as unpublished values also from the RECONS program for which final values will be presented in future papers in this series.

As shown in Figure 1, the median time coverage for stars in the sample is 7.9 years, with a broad distribution that stretches from 3.8 years to 14.0 years of observations for stars that were targeted at the beginning of the program. The primary focus of the program at the 0.9m involves the discovery and characterization of nearby stars, with most stars within 25 pc, but the set of stars presented here is by no means a complete, volume-limited sample. Target stars are usually selected based upon their high proper motions (Hambly et al. 2004; Subasavage et al. 2005a,b; Finch et al. 2007; Boyd et al. 2011a,b; Riedel et al. 2011) or photometric attributes (Henry et al. 2004; Winters et al. 2011) that indicate they are likely to

be closer than 25 pc. However, there are two groups of red dwarfs on the program that were eventually found to be at significantly different distances than anticipated. Cool subdwarfs (Jao et al. 2005, 2011) fall below the main sequence in the H-R diagram, and are closer than their photometric distance estimates imply. Young red dwarfs (Riedel et al. 2011, 2014) lie above the main sequence and are consequently further than their photometric distance estimates. Thus, the best assessment of variability rates in a census of stars includes a detailed analysis of their distances, to prevent over or underrepresentation of subsamples of stars that may bias the statistics. Of the 264 stars in the sample discussed here, 238 are known to be within 25 pc based on our trigonometric parallaxes. Below, we analyze both the entire list of stars observed and the restricted sample of only those within 25 pc.

3. Observations and Data Reduction

RECONS has been using the CTIO/SMARTS 0.9m telescope for astrometric and photometric observations since 1999, first as an NOAO Surveys Program, and since 2003 under the auspices of the SMARTS Consortium. The telescope is equipped with a 2048 x 2048 Tektronix CCD camera that is rarely moved, which provides the long-term astrometric stability needed for parallax work (Dieterich et al. 2014; Henry et al. 2006; Jao et al. 2005, 2011, 2014; Riedel et al. 2010, 2011, 2014; Subasavage et al. 2009) as well as a stable photometric platform. Images taken during the program are used here to investigate the photometric variability of the nearby M dwarfs that have been targeted for parallax and proper motion measurements. Observations are made using the central quarter of the chip, which provides a 6'8 square field of view and pixels 401 milliarcseconds in size. Parallax frames are taken in the V , R , and I filters² with magnitudes ranging from 9 to 20.

For astrometry, five images of each star are typically taken per night, usually within 30 minutes of transit. The target star is positioned in the field so that 5–10 reference stars, normally fainter by 1–4 magnitudes, surround the target. These stars constitute a reference grid for the astrometric reductions, and are also used for the photometric variability study described here. Additional details of the observations can be found in Jao et al. (2005). Exposure times usually range from 10–300 sec, with a few of the faintest stars requiring 600–900 sec integrations.

²The central wavelengths for the V_J , R_{KC} , and I_{KC} filters used in this study are 5438/5475, 6425, and 8075 Å, respectively. The two V filters used during this study have been found to be photometrically identical at a level better than the 7 mmag minimum level of our variability sensitivity, as there are no offsets observed in the more than 100 stars observed in the V band (Jao et al. 2011). The subscript “J” indicates Johnson, “KC” indicates Kron-Cousins (usually known as Cousins), and are hereafter omitted.

Data reduction includes calibration using flatfield and bias frames that are taken nightly. Each science frame is then manually checked for saturation of the target star or any reference stars. A frame with a saturated target star is discarded; individual reference stars are discarded if saturated, but the frame is used if sufficient reference stars remain available for reliable relative photometry.

VRI photometry from our program is given for the sample stars in Table 1. Details of the photometry observations and reductions can be found in Jao et al. (2005) and Winters et al. (2011). Briefly, calibration frames are taken nightly, and standard stars selected from Bessel (1990), Graham (1982), and Landolt (1992, 2007) are observed multiple times each night in order to derive transformation equations and extinction curves. Apertures 14'' in diameter were used to determine the stellar fluxes, except in cases where close contaminating sources needed to be deblended, in which case smaller apertures were used and aperture corrections were applied. Photometric errors for the *VRI* magnitudes are typically 0.03 mag, measured using (usually) multiple nights of data and taking into account extinction corrections for each night via standard star observations. These errors are much larger than the relative photometry for the variability measurements discussed below, which instead use stars in the target fields at virtually identical airmasses.

4. Variability Measurements

Here we define photometric variability to be the standard deviation of a star’s flux, measured in milli-magnitudes (mmag), when compared to a set of reference stars. Once a setup frame that positions a target star within an ensemble of reference stars has been established, the target star’s magnitude in each frame is compared to the reference stars using the methodology outlined in Jao et al. (2011). As an amendment to that methodology, we incorrectly stated in that paper that our instrumental magnitudes were based on counts within a defined aperture, whereas in fact they are based on Gaussian fits to the light distribution of each source. Briefly, we calculate instrumental magnitudes via SExtractor by integrating an object’s pixel values within a circular Gaussian profile that is scaled to an object’s image size and shape in a frame. The FWHM of this circle will be the radius of the disk that contains half of the object’s flux. We control for changes in seeing, airmass, and atmospheric transparency in a series of exposures for an object by utilizing the prescription discussed in Honeycutt (1992).

True stellar variability may be due to short-term flaring activity, mid-term rotation with spots, or long-term changes in spot numbers, i.e., a stellar cycle. Variability in frames due to other causes is identified and removed from the dataset. Such false variability may

be caused by frames compromised by high background because they were taken in twilight or moonlight, or by contamination by a nearby source as the proper motion of the target star causes its position to slide across the field. One of the advantages to this long-term program and its fairly high resolution images (401 milliarcsecond pixels) is that the positions of background sources can be identified and monitored over time relative to target stars, thereby eliminating contaminating sources. Finally, reference stars that do not fit the trend of instrumental magnitude standard deviation with brightness (see Jao et al. 2011, Figure 3) are removed from the analysis, and the target star’s brightness is compared to the remaining “quiet” reference stars.

For the stars discussed here, we find standard deviations in the photometric series as low as 6.4 mmag, although only a half dozen stars have standard deviations below 7 mmag, which we adopt as the one-sigma minimum deviation threshold. This matches the 7–8 mmag variability measured for three stars in Jao et al. (2011) with long time-series of images using two different V filters. Thus, mixing the two V filters is not a serious concern because the filters appear to be so similar that any offsets are much smaller than the 7 mmag minimum variability threshold we can measure. This level, which we refer to henceforth as the detectable “variability floor”, is represented with horizontal solid lines at 7 mmag in Figures 2–4. As a conservative measure of variability, we define significantly variable stars as those with standard deviations of 20 mmag or more relative to the chosen reference star set, but note that some stars in the 15–20 mmag range are variable at a lower level. This value is measured on an absolute scale, so that -20 mmag and $+20$ mmag differences would both be regarded as variability by 20 mmag.

5. Results

In Figures 2–4 we show photometric variability as functions of apparent VRI magnitude, $V - K_s$ color, and M_V . There are 114 stars observed in the V filter, 81 in the R filter, and 69 in the I filter.

In the three panels of Figure 2, there are no obvious trends in variability with apparent magnitude, but there are more stars variable by at least 20 mmag in V than in R or I . The intrinsically faintest, reddest, stars are typically observed in the I filter to boost S/N, and as discussed in §6, among the three filters this is where we find the least variability, as expected. Our variability floor of 7 mmag is the same in all three filters and at all brightnesses because we integrate for longer times on fainter targets to boost S/N for the astrometry studies, with the consequence that our photometric errors are not a strong function of brightness (Winters et al. 2011). We therefore conclude that systematic errors

concerning our lower limit of variability detection have been ameliorated, and that the overall observational thresholds for variability detection are consistent among the three filters and at various target brightnesses.

The three panels of Figure 3 show perhaps a subtle trend of long-term variability with $V - K$ color, which corresponds to temperature, with redder M dwarfs perhaps a bit more variable in V and R , but not in I , than early-type M dwarfs. However, this trend is weak, if present at all, and only with a much larger sample might the trend be confirmed. The three panels of Figure 4 are similar to those in Figure 3, now using absolute magnitudes to explore trends in luminosity rather than temperature. The results are predictably similar to Figure 3 because luminosity is linked to temperature for main sequence stars.

6. Discussion

Inspection of Figures 2–4 reveals a distribution of long-term variability in red dwarfs that we divide into two populations: (1) clearly variable stars that change brightness by more than 20 mmag, with a few stars highly variable at more than 50 mmag, and (2) those that are relatively quiescent with variability less than 20 mmag. The division at 20 mmag is used to compute the fractions of variable stars, illustrated using a restricted sample of stars in the histogram of Figure 5 (discussed below). As illustrated in Figures 6–8, there are some likely variable stars in the relatively quiescent group with variability measurements of 15–20 mmag, but our goal here is to understand what fraction of red dwarfs vary by a significant amount, here chosen to be a threshold of 20 mmag, or $\sim 2\%$ in flux in the observed bands. In the full sample, only 24 (9%) of the 264 stars vary photometrically by at least 20 mmag over long timescales; thus, $\sim 90\%$ of red dwarfs change in optical brightness by less than 2%. For the full sample, the fractions of stars that fall into the variable/quiescent groups are 18%/82% in the V band (114 stars), 4%/96% in the R band (81 stars), and 3%/97% in the I band (69 stars).

These fractions are subject to the biases of the observational program, which targets red dwarfs possibly within 25 pc. The primary bias of concern is the sample of young stars that are larger and intrinsically brighter than main sequence dwarfs, resulting in distance estimates placing them much closer than their true distances. There are 15 young stars, as determined by Riedel et al. (2014), in our sample, denoted with “Y” in Column (2) of Table 1, and with encircled points in Figures 2–4. Seven of these stars were observed in the V filter and eight in the R filter. Seven of the stars vary by more than 20 mmag (six in V and one in R), implying that 47% are variable stars by our criterion, a much higher fraction than in the sample as a whole.

Ideally, we would use a complete, volume-limited, sample to measure the fractions of red dwarfs photometrically variable over long timescales. Our best possible assessment with the current dataset is to restrict the sample to the 238 stars known to be within 25 pc via our trigonometric parallaxes, which is at least more representative of the red dwarf population than the full sample. Among these, the fractions of variable/quiescent red dwarfs are 13%/87% in the V band (106 stars), 4%/96% in the R band (70 stars), and 3%/97% in the I band (62 stars). Overall, only 19 of the 238 stars (8%) are variable by 20 mmag or more. We retain six young stars in the 25 pc sample (two observed at V and four at R) that vary by 17–25 mmag. All six stars vary by more than the median variability values in the V (14 mmag), R (13 mmag), and I filters (11 mmag).

Somewhat to our surprise, we do not see any strong trends in long-term variability with color (Figure 3) or luminosity (Figure 4) through the full range of red dwarfs in our sample. From the earliest types that have $V - K = 4.0$, $M_V \sim 10$, spectral type M2V, and $T = 3600\text{K}$, to those with $V - K = 9.2$, $M_V \sim 20$, spectral type M8V, and $T = 2200\text{K}$, (for empirical definitions of M dwarfs, see Henry et al. (1994), Baraffe & Chabrier (1996), Henry et al. (2006), and Dieterich et al. (2014)), there are no obvious trends in activity with stellar type seen in any of the VRI bands. This is a particularly revealing result — stars that differ by a factor of $\sim 10^4$ in visual flux (using M_V) and ~ 160 in total luminosity do not exhibit any trends in their photometric variability over long time periods in the bands where they exhibit a sizeable amount of flux. For example, M0V stars emit 46% of their flux in the VRI bands, in contrast to M5V stars that emit 17% in the same bands. Furthermore, because red dwarfs lose their radiative zones and become fully convective around $V - K \approx 4.5$, $M_V \approx 11.0$ (Chabrier & Baraffe 1997), we might also expect to see an abrupt change in long-term photometric variability character at that color and absolute magnitude. We do not see such a change in the current sample, but we have not observed many stars bluer than $V - K = 4.5$.

To evaluate the relative variability in the three bands, we restrict the 25 pc sample further to include only stars with $V - K = 4.5\text{--}6.5$, in order to limit the effects of fainter, redder, stars in the sample that are typically observed in the I filter. This subsample contains a total of 180 stars, with median variability values of 14 mmag at V (94 stars), 13 mmag at R (66 stars), and 11 mmag at I (20 stars). These values are unchanged from the analysis including stars of all colors within 25 pc, and we conclude that red dwarfs vary slightly more in the V and R bands than in the I band over multi-year timescales, confirming what we reported in Jao et al. (2011).

In Figure 5 we show the fractions of stars within 25 pc observed in V that are variable by more than 20 mmag, as a function of M_V . The range is restricted to only those bins that

have at least 10 stars, thereby including 97 of the 106 stars meeting the selection criteria. The error bars represent counting statistics and illustrate that more stars are needed to discern if there are any trends with luminosity — the total of 13 stars meeting our variability threshold is too small a sample to identify any trend.

7. Systems Worthy of Note

Here we provide details on several stars observed during the survey, grouped by type of variability and listed alphabetically within each group. Example plots of variability in the various categories are presented in Figures 6–8. We break the stars into those showing stellar cycles, trends, and erratic brightness changes likely due to spots and/or flares. We note that some of these stars do not formally exceed our conservative 20 mmag threshold for obvious variability, but they are highlighted here primarily because we see compelling trends in their data sets.

In the upper left panel of Figure 6, we first show a baseline non-variable target, **SCR 1845-6357AB**, which is composed of an M8.5V dwarf and a brown dwarf companion separated by $\sim 1''$ that does not affect the photometry. In fact, this target has such a low level of variability that we have adopted it as a red photometric standard.

Stellar Cycles in GJ 831AB, GJ 1061, LHS 2397aAB, LP 467-016AB, and SCR 0613-2742AB: These five targets exhibit cyclic variations in their photometry, illustrated in Figure 6. GJ 831AB is a fast-orbiting binary with an orbital period of 1.93 years and $\Delta V=2.1$ between the two components (Franz et al. 1997; Henry et al. 1999).³ We see a pattern in our current dataset with a period of ~ 8 yr, although there are deviations from a clear sinusoidal cycle in 2005. Given $\Delta V=2.1$, presumably the observed variability is in the primary component. The variation in GJ 1061 is muted, with a tentative cycle lasting about 8 years. The variations in LHS 2397aAB and LP 467-016AB appear to be robust, with periods of ~ 4 years and ~ 5 years, respectively. The most obvious cycle is that of SCR 0613-2742AB, for which we derive a period of ~ 0.4 years. Because of the short period for the cyclic behavior noted for SCR 0613-2742AB, we are likely seeing evidence of the rotation period, while the longer term upward trend may reflect a portion of a long-term cycle.

Photometric Trends in G 169-029, GJ 876, L 449-001AB, LHS 1610AB, LHS 2021, and WT 460AB: These six targets show long-term trends in their photometry, illus-

³A possible third component mentioned in those papers has not been confirmed through continued work on the dataset, so the system is a binary, not a triple.

trated in Figure 7, but have not yet clearly completed a cycle in our coverage. Remarkably, G 169-029 (10 years) and WT 460AB (13 years), show extraordinarily long-term trends that have yet to invert, with overall flux changes of $\sim 5\%$ in R and I , respectively. To our knowledge, these are the first discoveries of changes in red dwarf fluxes lasting a decade or more. WT 460AB is a binary composed of two red dwarfs with spectral types M5.5V and \sim L1V separated by $0''.5$ (Montagnier et al. 2006). The large $\Delta H=2.5$ mag difference implies an even larger ΔI , so presumably the change in brightness is due to the M dwarf. The data series on L 449-001AB similarly shows a long-term trend throughout the 5-year time series in-hand. Additional trends are seen in the data for G 161-071, LHS 547, and SCR 2036-3607 (not shown here).

Spots in GJ 2006A, LP 932-083, and TWA 8A: These targets show distinctive variability illustrated in the left three panels of Figure 8, at levels of 77 mmag, 46 mmag, and 79 mmag, respectively. The data indicate that these stars change their broadband fluxes frequently, likely because much of the stellar surface is active with flares and/or spots. Flares and spots are both modulated by stellar rotation, as the active regions rotate in/out of our view, and as the spots change over long time periods. We do not see obvious cyclic patterns in the brightnesses of these three stars. The case of TWA 8AB is particularly intriguing. This is a binary member of the TW Hydra Association separated by 13 arcseconds, in which the A component shows clear spot activity and for which we have observed a flare in the B component (see below). Additional evidence for spots is seen in the data for G 007-034, G 131-026, GJ 1123, GJ 1284AB, GJ 2006B, LHS 2206, LHS 5094, LP 834-032, and Proxima Centauri (not shown here).

Flares in GJ 1207, LHS 6167AB, and TWA 8B: These three stars show clear flare events, illustrated in the right panels of Figure 8. GJ 1207 has the largest variability measurement, 196 mmag, in the sample, caused entirely by our observation of a flare that brightened the star by 1.7 mag in V on UT 2002 June 17 (Henry et al. 2006). Omitting the flare event reduces its variability to 18 mmag. LHS 6167AB shows a flare with amplitude 0.2 mag on UT 2013 April 2. TWA 8B is the second most variable star in our sample, at 124 mmag, again caused by single 0.7 mag flare in V observed on UT 2000 March 27.

Overall, there are only four red dwarfs in the sample that vary by more than 50 mmag: GJ 1207, GJ 2006A, TWA 8A, and TWA 8B, all observed in the V filter. The GJ 2006 (the B component varies by 36 mmag in V) and TWA 8 systems are young stars, as discussed in Riedel et al. (2014). GJ 1207 is not known to be a young system, and without the single extreme flare event mentioned above, it would fall in our quiescent group.

8. Comparison to Previous Studies

8.1. Long-Term Results from Ground-Based Studies

In his classic study, Weis (1994) used a GaAs photomultiplier tube and a similar *VRI* filter set to that used in our study. Although Weis was not able to guarantee the same tube and filter set for every run (typically seven to eight nights, which he referred to as a season of observation), he provided valuable results on the variability of nearby M dwarfs. He observed 43 stars for up to 11 years in all three of the *VRI* filters, and determined a variability detection limit of 5 mmag for his observational technique. Weis used σ_a to denote the average mean error of a seasonal mean magnitude and σ_b to denote the dispersion of the seasonal mean magnitudes about the overall mean. These two quantities correspond to short-term (over a \sim week) and long-term (over years) variability measurements. He concluded that 21 of the stars exhibited long-term variability at the 95% confidence level. However, most of the variability was in the range 10-20 mmag; only 8 (19%), 4 (9%), and 0 (0%) stars were variable at the 20 mmag level over long time periods in the *V*, *R*, and *I* bands, respectively. Our variability measurements are similar to Weis’ σ_b measurement, and we find similar fractions of variability, albeit for \sim six times the number of stars: 18%, 4%, and 3% of our stars vary by more 20 mmag or more at *V*, *R*, and *I*, respectively. To our knowledge, Weis’ work is the first significant study of the long-term variability of red dwarfs.

Jao et al. (2011) studied a set of 22 cool subdwarfs, and compared them to 108 main sequence red dwarfs. Those results are based on the same long-term astrometry/photometry taken during the RECONS program at the 0.9m outlined above, but over a somewhat shorter time period. For the first time, that study revealed that red subdwarfs are less photometrically variable in the *VRI* bands than their main sequence counterparts, with average variabilities for the 22 cool subdwarfs at levels of only 7 mmag at *V* (3 stars), 8 mmag at *R* (13 stars), and 7 mmag at *I* (6 stars). This is effectively the variability floor level of our observations, and in fact, cool subdwarfs are likely even less variable than indicated by those values.

Spectroscopic variability studies of M dwarfs spanning years have been carried out by Gomes da Silva et al. (2012) and Robertson et al. (2013). Both studies focused primarily on stars with spectral types M0V–M4V, a bluer set of stars than our M2V–M8V sample. Gomes da Silva et al. (2012) investigated 27 M dwarfs in the HARPS radial velocity program with a median observational timespan of 5.9 years to detect correlations between long-term activity variations and the measured radial velocities. By using the NaI D doublet as an activity index, they found that 14 of the stars had activity indicative of long-term variations, although in truth, only a few of the NaI vs. time plots show convincing cycles. Assuming

their selection of the five stars deemed to have reliable sinusoidal signals in their NaI indices, their variable activity rate is 19%.

In a comparable spectroscopic study, Robertson et al. (2013) used ~ 11 years of spectra from the McDonald Observatory M Dwarf Planet Search to reveal cyclic variations in M dwarfs that could be measured using the $H\alpha$ line. Among their 93 stars they identified five exhibiting periodic signals ranging from 0.8–7.4 years, and found eight additional stars showing long-term trends, or at least offsets in $H\alpha$ index over time. Their fraction of stars with detected changes in $H\alpha$, 14%, is similar to our fraction of stars varying by more than 20 mmag in the V band, 18%, implying that changes in $H\alpha$ may correlate quite well to changes in V band flux.

The single star included in Gomes da Silva et al. (2012), Robertson et al. (2013), and our study is the multi-planet system GJ 581. The spectroscopic studies report periodic signals in NaI lasting 3.9 years in a 6-year dataset and in $H\alpha$ lasting 4.5 years in a 9-year dataset, respectively. GJ 581 falls in the quiescent set of our stars, varying by only 13 mmag in V over 12.8 years. We note that GJ 581 has the largest false alarm probability (0.12) of the five stars with periodic signals in Robertson et al. (2013), and although Gomes da Silva et al. (2012) state that this is the star with the highest probability that its activity data can be fitted with a sinusoidal signal, the amplitude is only twice the average error. We conclude that this particular cycle may not be real. Nonetheless, long-term photometric monitoring of GJ 581 and the other NaI and $H\alpha$ variable stars would certainly be a worthy project, particularly at the ~ 1 mmag level possible with ground-based telescopes.

8.2. Shorter-Term Results from Ground-Based Studies

Hartman et al. (2011) explored the optical variability of a sample of 27560 field K and M dwarfs using data from the HATNet transit-search survey. Their observational series range from 45 days to 2.5 years, with a median time span of half a year. Thus, they are sampling time periods suited for exploring rotation periods, rather than the stellar cycles we are investigating. After carefully deleting blended sources, a concern because of HATNet’s 9–14"/pixel scales, they find 1490 stars (excluding eclipsing binaries) that vary at the 10 mmag level in the RI bands, indicating that at least $\sim 5\%$ vary at this level. In their Figure 14, they show an increasing fraction of variable stars with $V - K$ color. For stars having $V - K = 4.5\text{--}6.5$, like most of those in our study, they find 10 mmag variability rates rising from 7% to more than 40%, although the error bars are significant, particularly beyond $V - K = 5.25$ because there are 20 or fewer stars in each of those three bins. Regardless, this large survey indicates that most M dwarfs *do not* vary by more than 1% over many

months, similar to our conclusion for similar stars over many years.

Irwin et al. (2011) reported rotation periods, based upon photometric variability, in the range of a few hours up to about 5 months for 41 red dwarfs from the MEarth project. Their study differs from that of Hartman et al. (2011) in that they were specifically targeting nearby stars, and using much higher resolution images, with pixels $0.76''$ in size so blending is rarely an issue. As with the HATnet survey, their observations are higher cadence than ours, with typically several hundred to several thousand observations per star over time periods of 3 months to 3 years, with an upper sensitivity limit to periodicities at 5 months. The observations were made through a long pass filter at 715 nm, and periodic variations were reported with amplitudes of 2.7 to 23.9 mmag in their Table 1. Their study does not examine the long-term variability discussed here, but as with Hartman et al. (2011), provides important complementary information. The 41 stars with rotation periods were extracted from an overall sample of 273 stars, of which $\sim 80\%$ had at least 100 observations on 10 or more nights, indicating that $\sim 20\%$ of the well-sampled stars had determinable rotation periods. Among these, 10 have semi-amplitudes of at least 10 mmag, or roughly 5%, similar to that found by Hartman et al. (2011), although no information was provided about the variability rate for stars not found to have rotation periods.

Finally, Koen et al. (2010) reported *UBVRI* photometry for over 700 nearby stars, primarily of spectral types K and M. Their study is rather different than ours, as it was an effort to provide photometry, with typically a handful of observations per star rather than long time series over many years. Nonetheless, as outlined in their Figure 3 (based on apparent *V* magnitude), they find that most of their sample stars vary by less than 20 mmag, similar to our result.

8.3. Results from the Kepler Mission

To date, the Kepler mission has provided an opportunity to study a few thousand M dwarfs in the northern hemisphere photometrically, although most are not in the immediate solar neighborhood, and none are in common with the stars studied here. Kepler samples the light curves of stars in a bandpass that spans 400-850 nm, every 30 minutes for the datasets discussed here. This single bandpass roughly corresponds to the combined light of the *VRI* bands we have used.

In a study of the first month of Q1 Kepler science data, Ciardi et al. (2011) extracted variability rates for periods up to 33 days for 129,000 dwarfs, including more than 2000 identified as M dwarfs. There are two apparent magnitude samples examined that provide

useful statistics, but there are several *caveats*: the stars are at various distances, sources are defocused so may be unresolved multiple systems or blends with background stars, and while significant efforts were made to separate the dwarfs and giants, no color information for individual stars is given, so various types of M dwarfs (and possibly other red objects) were mixed in the samples. Using data in their Table 2, for M dwarfs having $M_{Kepler} = 12\text{--}14$, 14 of 154 stars (9%) had magnitude dispersions greater than 10 mmag over the 33 day period. For $M_{Kepler} = 14\text{--}16$, 150 of 2182 stars (7%) varied by 10 mmag. In addition, they find that the overall variability fraction at the 30-minute sampling rate increases for the M dwarfs as baselines increase from 1 to 33 days, and therefore conclude that M dwarfs vary primarily on timescales of weeks or longer. Because our variability floor is 7 mmag, a direct comparison to the results from Kepler, which measures photometry to tens of parts per million, is problematic — we find that 193 (73%) of the 264 stars in our sample vary by at least 10 mmag in one of the three *VRI* filters, but this large fraction is simply because 10 mmag is very close to our variability floor.

In a second Kepler study, Walkowicz et al. (2011) examined $\sim 23,000$ K and M dwarfs in the same Q1 dataset as Ciardi et al. (2011), again using the 30-minute cadence results over a 33 day time period, with the goal of identifying flare stars. They found 373 stars that exhibited flare activity via their EW_{phot} parameter. They derive three characteristics of the stars in their flare sample: (1) M dwarfs flare more frequently than K dwarfs, but for shorter durations, (2) there is no dependence on the flare peaks with stellar effective temperature, and (3) stars that have larger quiescent variability have intrinsically larger flares. Overall, the fraction of stars exhibiting flares in the Kepler dataset is very low, less than 2%. This is consistent with our data, given that we have identified only three stars that clearly flare among 264.

More recently, Hawley et al. (2014) report flare occurrence rates for five M dwarf systems (four singles and one close double) monitored by Kepler in short cadence mode. Three of the M dwarfs had no H α emission and were labeled “inactive”, yet still produced a few energetic flares, but at much lower rates than their active counterparts. These three inactive M dwarfs were in flaring states for 0.1%, 0.6%, and 1.5% of the time observed, while the two active M dwarf systems spent 27% and 36% of the time in a flaring state. Thus, chromospherically inactive M dwarfs do exhibit energetic flares, but only rarely, which is consistent with the very few flares we have seen in more than a decade of monitoring nearby red dwarfs.

8.4. Summary of Results

The long term efforts of Weis (1994), Jao et al. (2011), Gomes da Silva et al. (2012), and Robertson et al. (2013), as well as our study presented here, all indicate that only ~ 10 – 20% of red dwarfs vary by at least 2% in the V band, or when using proxy spectral features. At R and I , the variability rate is much lower. In sum, these studies clearly indicate that M dwarfs do exhibit long-term cycles like our Sun, but that most M dwarfs do not vary by more than a few percent over long timespans.

The remaining optical wavelength studies discussed here focus on timespans suited to determining rotation periods, rather than stellar cycles. Those results explore timescales up to a few months in duration, whereas our measurements are over years, yet in sum also indicate that only a small fraction of M dwarfs exhibit flux variability exceeding a few percent. Although the VRI bands in which we have observed the stars in this survey may not be those in which variability is greatest, such as at x-ray wavelengths, red dwarfs emit much of their flux in these bands, in particular for the earlier types. Most of the rest of red dwarfs’ flux is emitted in the near-infrared, and the study by Goulding et al. (2012) of ~ 9600 M dwarfs yielded only 68 stars (less than 1%) that were periodically variable by more than 10 mmag (their Table A1) in the J band. This is a much smaller fraction than we found at VRI , and confirms the trend of less variability with increasing wavelength.

9. M Dwarf Variability and Exoplanets

One of the motivations for this study was to evaluate the variability of the ubiquitous red dwarfs because such variations will affect the environments, and perhaps the habitability, of any orbiting planets. In particular, long-term variations in the flux emitted could affect planetary atmospheres in ways similar to how our Sun affects the Earth’s atmosphere, e.g., the cyclic influx of charged particles that cause aurorae and expansion/contraction of the atmosphere. Here we discuss some of the nearest red dwarfs with detected exoplanets to provide context for effects on planetary environments that stretch over years.

In Table 2, we list M dwarfs within 25 pc currently reported to have orbiting exoplanets. This sample has been created using the intersection of the exoplanets.org and exoplanet.eu websites as of 01 July 2014 — stars are only included if the detected exoplanets have been vetted and listed by both groups. The sample is heavily skewed to the closest M dwarfs; presumably many more planets await discovery within 25 pc. We list the number of reported planets and photometry for the 17 stars, as well as our own monitoring results for seven stars, including VRI photometry, filters used for the long-term observations, the variability

levels, and the duration and number of observations (nights, frames). The unobserved stars in Table 2 are not being followed because they are either too bright for our astrometric program, requiring short exposures and consequently poor centroids for astrometry, or are in the northern sky.

None of the seven exoplanet host stars we have observed has been found to be variable by more than 20 mmag in the available datasets. The only star of note among the seven is GJ 876, which displays a possible stellar cycle (Figure 7), growing brighter from 2004–2006, and rather fainter in the most recent epoch available in 2013. We conclude that photometric variability, at least at optical wavelengths, is not a concern for the environments of exoplanets orbiting most red dwarfs.

10. Conclusions

We have collected photometric observations for 264 red dwarfs over the past 14 years, with a median duration in the coverage of 7.9 years. We have used these images to determine long-term photometric variability in the *VRI* bands, and reach the following conclusions:

- Only $\sim 10\%$ of red dwarfs are variable at the 20 mmag level over multi-year timescales in the *VRI* photometric bands. Thus, the impression that red dwarfs are highly active with large changes in brightness is likely due to the notoriety of a small number of highly variable stars, e.g. EV Lac. Instead, most red dwarfs are relatively quiet, at least at optical wavelengths.
- As expected, we find that the measured variability is lower in the *I* band than in the *V* or *R* bands. Of the 25 stars varying by more than 20 mmag, 20 were observed in the *V* band. Given that most red dwarfs emit the majority of their flux in the *I* band, or at even longer wavelengths in the near-infrared where the variability is even lower, the overall fluxes of most red dwarfs change very little.
- To our surprise, we find no clear trends in variability at the 20 mmag level for M dwarfs as functions of luminosity or temperature, at least in the current sample. However, identifying relatively young stars can be accomplished via long-term photometric monitoring.
- We have identified several red dwarfs exhibiting long-term photometric changes, including five stars with cyclic periods lasting up to 8 years and nine stars with long-term trends, two of which have been continuing for a decade. At least 12 additional stars show evidence of spots.

These results have a particular application to the study of habitable environments

around M dwarfs. To first-order, planetary surface temperatures are estimated based on the stellar flux and the distance of a planet from its host star. Here we investigate a second-order effect over \sim decade timescales: the *change* in insolation as an M dwarf varies may be crucial for planetary environmental impact. We find that $\sim 90\%$ of M dwarfs vary by less than 2% at wavelengths where they emit much of their light, implying that long-term flux levels do not change appreciably on most planets orbiting red dwarfs.

To further refine the fractions of variables in the red dwarf population, future studies should target larger, volume-limited samples. This would reduce concerns related to biases in the current sample, including the overabundance of active young stars and unresolved multiples that have been treated as single stars. In addition, more refined studies could probe to higher precision. For example, the CTIO/SMARTS 0.9m telescope used to make the observations discussed here is able to reach photometric precisions of ~ 1 mmag when target stars are defocused to boost the total stellar signals, compared to the 7 mmag variability floor achieved here using the tightly focused images required for astrometry. Nonetheless, we now know that most red dwarfs, which comprise three-quarters of all stars in the solar neighborhood, are photometrically stable on decade timescales at a level of 2% at optical wavelengths. This bodes well for the stability of environments on any planets that might be orbiting them.

11. Acknowledgments

ADH thanks the McNair Fellowship program under the support of TRIO for providing funding for this research. The RECONS effort has been supported by the National Science Foundation through grants AST 05-07711, AST 09-08402, and AST 14-12026. We also thank the members of the SMARTS Consortium and the CTIO staff, who enable the operations of the small telescopes at CTIO. This research has made use of results from the SAO/NASA Astrophysics Data System Bibliographic Services, as well as the SIMBAD and VizieR databases operated at CDS, Strasbourg, France, and the Two Micron All Sky Survey, which is a joint project of the University of Massachusetts and the Infrared Processing and Analysis Center, funded by NASA and NSF.

REFERENCES

- Baraffe, I., & Chabrier, G. 1996, *ApJ*, 461, L51
- Bessel, M. S. 1990, *A&AS*, 83, 357
- Boyd, M. R., Henry, T. J., Jao, W.-C., Subasavage, J. P., & Hambly, N. C. 2011b, *AJ*, 142, 92
- Boyd, M. R., Winters, J. G., Henry, T. J., et al. 2011a, *AJ*, 142, 10
- Chabrier, G., & Baraffe, I. 1997, *A&A*, 327, 1039
- Ciardi, D. R., von Braun, K., Bryden, G., et al. 2011, *AJ*, 141, 108
- Davison, C. L. et al. 2014, *AJ*, 147, 26
- Dieterich, S. B., Henry, T. J., Jao, W.-C., et al. 2014, *AJ*, 147, 94
- Finch, C. T., Henry, T. J., Subasavage, J. P., Jao, W.-C., & Hambly, N. C. 2007, *AJ*, 133, 2898
- Franz, O. G., Wasserman, L. H., Henry, T. J., et al. 1997, *Bulletin of the American Astronomical Society*, 29, 1361
- Gomes da Silva, J., Santos, N. C., Bonfils, X., et al. 2012, *A&A*, 541, A9
- Goulding, N. T., Barnes, J. R., Pinfield, D. J., et al. 2012, *MNRAS*, 427, 3358
- Graham, J. A. 1982, *PASP*, 94, 244
- Hambly, N. C., Henry, T. J., Subasavage, J. P., Brown, M. A., & Jao, W. C. 2004, *AJ*, 128, 437
- Hartman, J. D., Bakos, G. Á., Noyes, R. W., et al. 2011, *AJ*, 141, 166
- Hawley, S. L. et al. 2014, *ApJ*, 797, 121
- Henry, T. J., Franz, O. G., Wasserman, L. H., et al. 1999, *ApJ*, 512, 864
- Henry, T. J., Jao, W. C., Subasavage, J. P., Beaulieu, T. D., Ianna, P. A., Costa, E., & Mendez, R. A. 2006, *AJ*, 132, 2360
- Henry, T. J., Kirkpatrick, J. D., & Simons, D. A. 1994, *AJ*, 108, 1437

- Henry, T. J., Subasavage, J. P., Brown, M. A., Beaulieu, T. D., Jao, W. C., & Hambly, N. C. 2004, *AJ*, 128, 2460
- Honeycutt, R. K. 1992, *PASP*, 104, 435
- Irwin, J., Berta, Z. K., Burke, C. J., et al. 2011, *ApJ*, 727, 56
- Jao, W.-C., Henry, T. J., Subasavage, J. P., Brown, M. A., Ianna, P. A., Bartlett, J. L., Costa, E., & Méndez, R. A. 2005, *AJ*, 129, 1954
- Jao, W.-C., Henry, T. J., Subasavage, J. P., et al. 2011, *AJ*, 141, 117
- Jao, W.-C., Henry, T. J., Subasavage, J. P., et al. 2014, *AJ*, 147, 21
- Koen, C., Kilkeny, D., van Wyk, F., & Marang, F. 2010, *MNRAS*, 403, 1949
- Landolt, A. U. 1992, *AJ*, 104, 372
- Landolt, A. U. 2007, *AJ*, 133, 2502
- Lurie, J. C., Henry, T. J., Jao, W.-C., et al. 2014, *AJ*, 148, 91
- Mamajek, E. E., Bartlett, J. L., Seifahrt, A., et al. 2013, *AJ*, 146, 154
- Montagnier, G., Ségransan, D., Beuzit, J.-L., et al. 2006, *A&A*, 460, L19
- Riedel, A. R., Finch, C. T., Henry, T. J., et al. 2014, *AJ*, 147, 85
- Riedel, A. R., Murphy, S. J., Henry, T. J., et al. 2011, *AJ*, 142, 104
- Riedel, A. R., Subasavage, J. P., Finch, C. T., et al. 2010, *AJ*, 140, 897
- Robertson, P., Endl, M., Cochran, W. D., & Dodson-Robinson, S. E. 2013, *ApJ*, 764, 3
- Subasavage, J. P., Henry, T. J., Hambly, N. C., Brown, M. A., & Jao, W.-C. 2005a, *AJ*, 129, 413
- Subasavage, J. P., Henry, T. J., Hambly, N. C., et al. 2005b, *AJ*, 130, 1658
- Subasavage, J. P., Jao, W.-C., Henry, T. J., et al. 2009, *AJ*, 137, 4547
- Walkowicz, L. M., Basri, G., Batalha, N., et al. 2011, *AJ*, 141, 50
- Weis, E. W. 1994, *AJ*, 107, 1135
- Weis, E. W. 1996, *AJ*, 112, 2300

Winters, J. G., Henry, T. J., Jao, W.-C., Subasavage, J. P., Finch, C. T., & Hambly, N. C.
2011, AJ, 141, 21

Winters, J. G., Henry, T. J., Lurie, J.C., et al. 2015, AJ, 149, 5

Table 1. Red Dwarfs Studied for Long-Term Variability

Name	Young	R.A. J2000.0	Dec. J2000.0	<i>V</i>	<i>R</i>	<i>I</i>	Ref.	<i>K_s</i>	<i>V</i> − <i>K_s</i>	Filter	Variability (mmag)	Timespan	Duration (yr)	#Nights	#Frames	$\pi_{trig} \pm \sigma$ (mas)	Ref.
(1)	(2)	(3)	(4)	(5)	(6)	(7)	(8)	(9)	(10)	(11)	(12)	(13)	(14)	(15)	(16)	(17)	(18)
GJ 1001A	...	00 04 36	−40 44 02	12.83	11.62	11.08	Win15	7.74	5.09	R	13.7	1999.64-2011.74	12.10	21	112	77.02 2.07	Die14
GJ 1002	...	00 06 43	−07 32 17	13.84	12.21	10.21	Win15	7.44	6.40	R	13.9	2003.77-2012.87	9.10	14	64	207.18 3.09	Dav14
L 217-028	...	00 08 17	−57 05 52	12.13	11.00	9.57	Win15	7.40	4.73	V	9.8	2000.50-2008.00	7.25	15	68
G 131-026	...	00 08 53	+20 50 25	13.52	12.19	10.50	Rie14	8.01	5.51	V	18.9	1999.71-2011.89	12.18	21	97	54.13 1.35	Rie14
GJ 1005AB	...	00 15 28	−16 08 01	11.48	10.27	8.70	Win15	6.39	5.09	V	8.2	2003.75-2011.90	7.96	22	95
GJ 2006A	Y	00 27 50	−32 33 06	12.95	11.79	10.29	Rie14	8.01	4.94	V	76.8	2000.57-2010.82	10.25	17	69	30.14 2.50	Rie14
GJ 2006B	Y	00 27 50	−32 33 23	13.25	12.04	10.48	Rie14	8.12	5.13	V	36.2	2000.57-2010.82	10.25	17	69	31.78 2.47	Rie14
GR 50	...	00 32 53	−04 34 07	13.97	12.68	11.00	Win15	8.35	5.62	R	13.0	2007.82-2012.95	5.13	11	59
LHS 1140	...	00 44 59	−15 16 17	14.18	12.88	11.19	Win15	8.82	5.36	V	12.2	2003.95-2011.88	7.93	12	52
L 087-002	...	00 57 12	−64 15 24	12.40	11.28	9.81	Win15	7.60	4.80	V	8.9	2008.86-2012.87	4.01	14	70
GJ 1025	...	01 00 56	−04 26 56	13.35	12.08	10.52	Win15	8.22	5.13	V	19.8	2000.57-2012.75	12.17	13	66	87.70 2.38	Jao05
SCR 0103-5515ABC	Y	01 03 35	−55 15 56	15.48	14.00	12.07	Rie14	9.24	6.24	R	15.4	2007.82-2012.87	5.05	11	49	21.18 1.37	Rie14
L 087-010	...	01 04 06	−65 22 27	13.98	12.63	10.95	Win15	8.53	5.45	V	13.9	2008.64-2012.88	4.24	10	44
GJ 54AB	...	01 10 22	−67 26 41	9.82	8.70	7.32	Win15	5.13	4.69	V	16.4	2000.75-2012.00	11.20	40	197	141.20 3.38	Hen06
LP 467-016AB	Y	01 11 25	+15 26 21	14.46	12.95	11.03	Rie14	8.21	6.25	R	19.2	1999.71-2009.57	9.86	15	79	45.79 1.78	Rie14
LEHPM 1-1343	...	01 13 16	−54 29 13	14.16	12.85	11.17	Win15	8.68	5.48	R	21.3	1999.91-2004.98	5.06	14	64
GJ 2022B	Y	01 24 30	−33 55 01	15.50	14.09	12.33	Rie14	9.68	5.82	R	14.4	1999.62-2011.53	11.91	16	66	38.80 2.13	Rie14
L 002-060	...	01 29 20	−85 56 11	13.49	12.21	10.58	Win15	8.08	5.41	I	6.7	2003.95-2008.70	4.75	10	55
LP 991-084	...	01 39 21	−39 36 09	14.48	12.97	11.06	Win15	8.27	6.21	V	14.2	2003.94-2012.96	9.02	14	66
L 294-092	...	01 47 42	−48 36 05	12.42	11.23	9.72	Win15	7.45	4.97	R	9.2	2004.75-2012.00	6.99	23	63
LHS 1302	...	01 51 04	−06 07 05	14.49	13.00	11.17	Win15	8.55	5.94	R	11.8	1999.71-2011.78	12.06	31	178	100.78 1.89	Hen06
LHS 5045	...	01 52 51	−48 05 41	13.79	12.48	10.80	Win15	8.24	5.55	R	9.4	2004.00-2008.80	5.67	20	44
SIP 0152-6329	...	01 52 55	−63 29 30	15.41	13.93	12.01	*	9.26	6.15	R	16.4	2007.82-2012.94	5.12	8	41
L 088-043	...	01 53 37	−66 53 34	11.68	10.60	9.24	Win15	6.99	4.69	R	8.1	2005.71-2011.89	6.18	15	79
L 173-019	...	02 00 38	−55 58 04	11.90	10.70	9.15	*	6.77	5.13	V	19.8	2007.81-2011.96	4.15	11	57
LHS 1339	...	02 05 48	−30 10 36	12.18	11.07	9.69	Win15	7.56	4.62	V	9.1	2004.00-2008.90	4.93	25	36
GJ 85	...	02 07 23	−66 34 11	11.49	10.49	9.31	Win15	7.36	4.13	V	9.2	2003.95-2012.70	8.75	14	69
LHS 1351	...	02 11 18	−63 13 41	12.23	11.15	9.82	Rie10	7.73	4.50	V	8.7	2000.58-2004.98	4.40	12	68	71.53 1.64	Rie10
LHS 1358	...	02 12 54	+00 00 16	13.58	12.31	10.66	Rie10	8.17	5.41	R	15.1	1999.71-2003.86	4.15	11	58	65.27 2.07	Rie10
LHS 1363	...	02 14 12	−03 57 43	16.44	14.71	12.62	Win15	9.49	6.95	I	11.1	2003.94-2012.95	9.01	17	64
G 075-035	...	02 41 15	−04 32 17	13.79	12.48	10.77	Win15	8.25	5.54	R	10.1	2003.95-2012.94	8.99	16	73
LP 993-115A	...	02 45 10	−43 44 32	12.38	11.17	9.61	Rie14	7.20	5.18	V	21.0	1999.62-2012.95	13.32	15	71	89.62 1.73	Rie14
LP 993-115BC	...	02 45 14	−43 44 10	12.69	11.37	9.67	*	7.27	5.42	V	14.5	1999.62-2012.95	13.32	15	71	84.12 2.08	Rie14
SCR 0246-7024	...	02 46 02	−70 24 06	14.86	13.44	11.61	Win11	9.02	5.84	R	12.6	2006.87-2012.94	6.07	12	51
SO 0253+1652	...	02 53 00	+16 52 52	15.14	13.03	10.65	Hen06	7.59	7.55	I	7.7	2003.53-2009.04	5.50	19	118	260.63 2.69	Hen06
LHS 1491	...	03 04 04	−20 22 43	12.84	11.65	10.13	Rie10	7.75	5.09	V	17.9	1999.71-2005.00	5.29	15	70	67.28 1.25	Rie10
LEHPM 1-3070	...	03 06 11	−36 47 52	19.38	16.98	14.49	Die14	10.63	8.75	I	8.5	2009.75-2013.80	4.06	11	54	76.46 1.42	Die14
LP 831-045	...	03 14 18	−23 09 29	12.58	11.42	9.93	Win15	7.63	4.95	V	16.6	2003.95-2011.77	7.82	20	60
LHS 1550	...	03 28 48	−27 19 04	13.75	12.58	11.07	*	8.77	4.98	R	13.9	2008.86-2012.94	4.08	11	57
LP 888-018	...	03 31 30	−30 42 38	18.81	16.55	14.10	Win15	10.26	8.55	I	9.0	2003.95-2012.88	8.93	15	69
LEHPM 1-3396	...	03 34 12	−49 53 32	19.38	16.85	14.39	Win15	10.39	8.99	I	8.4	2004.75-2012.93	8.18	20	95
LHS 1561	...	03 34 39	−04 50 33	13.07	11.84	10.30	Rie10	7.93	5.14	V	7.8	2000.07-2010.97	10.91	14	72	34.20 1.72	Rie10
LHS 176	...	03 35 38	−08 29 22	15.92	14.30	12.31	Jao11	9.46	6.46	I	9.7	2004.00-2009.10	5.17	17	47	77.77 1.30	Jao11
GJ 1061	...	03 36 00	−44 30 46	13.09	11.45	9.46	Hen06	6.61	6.48	R	15.2	1999.62-2012.95	13.32	31	194	271.92 1.34	Hen06
SCR 0336-2619	...	03 36 31	−26 19 57	16.33	14.76	12.72	*	9.76	6.57	I	10.8	2008.70-2012.94	4.23	7	39
LP 944-020	...	03 39 35	−35 25 43	18.70	16.39	14.01	Die14	9.55	9.15	I	8.8	2003.95-2012.94	8.99	14	59	155.89 1.03	Die14
SCR 0342-6407	...	03 42 57	−64 07 56	16.01	14.65	12.89	Jao11	10.58	5.43	I	7.0	2003.94-2007.89	3.95	12	66	41.56 2.01	Jao11
LHS 1582AB	...	03 43 22	−09 33 50	14.69	13.33	11.60	Rie10	8.85	5.84	R	14.6	2000.87-2012.70	11.82	22	92	50.84 1.21	Lur14

Table 1—Continued

Name	Young	R.A. J2000.0	Dec. J2000.0	V	R	I	Ref.	K_s	$V - K_s$	Filter	Variability (mmag)	Timespan	Duration (yr)	#Nights	#Frames	$\pi_{trig} \pm \sigma$ (mas)	Ref.
(1)	(2)	(3)	(4)	(5)	(6)	(7)	(8)	(9)	(10)	(11)	(12)	(13)	(14)	(15)	(16)	(17)	(18)
GJ 1065	...	03 50 44	−06 05 41	12.82	11.60	10.04	Win15	7.75	5.07	V	13.5	2003.95-2012.95	9.00	15	86	101.63 1.93	Dav14
LHS 1610AB	...	03 52 41	+17 01 04	13.85	12.42	10.66	*	8.05	5.80	V	27.4	1999.71-2009.93	10.22	24	142	101.57 2.07	Hen06
LHS 1630AB	...	04 07 20	−24 29 13	12.38	11.22	9.68	Rie10	7.44	4.94	V	8.9	1999.71-2009.03	9.32	22	137	56.18 1.06	Rie10
LP 889-037	...	04 08 55	−31 28 54	14.56	13.21	11.48	Win15	8.82	5.74	R	10.1	2003.95-2012.94	8.99	15	63
GJ 1068	...	04 10 28	−53 36 08	13.60	12.18	10.42	Jao05	7.90	5.70	R	9.0	1999.64-2009.93	10.29	29	194	143.42 1.92	Jao05
G 007-034	Y	04 17 18	+08 49 22	13.84	12.50	10.75	Rie14	8.18	5.66	R	24.1	1999.64-2007.83	8.19	15	72	73.27 1.27	Rie14
LHS 1656	...	04 18 51	−57 14 01	13.29	12.18	10.84	Rie10	8.65	4.64	I	8.4	2003.95-2009.74	5.08	13	51	39.41 1.94	Rie10
LHS 5094	...	04 26 32	−30 48 01	14.17	12.73	10.99	Win15	8.41	5.76	V	21.7	2003.95-2012.95	9.00	16	66
2MA 0429-3123	...	04 29 18	−31 23 56	17.39	15.50	13.32	*	9.77	7.62	R	18.8	2003.95-2012.95	8.99	16	69
LHS 1678	...	04 32 42	−39 47 12	12.48	11.46	10.26	Win15	8.26	4.22	V	6.4	2003.95-2012.10	8.14	14	70
LP 775-031	...	04 35 16	−16 06 57	17.67	15.49	13.08	Die14	9.35	8.32	I	8.1	2003.95-2012.88	8.94	19	74	95.35 1.06	Die14
LP 834-032	...	04 35 36	−25 27 34	12.44	11.26	9.73	Win15	7.41	5.03	V	42.0	2003.95-2011.74	7.79	13	64
G 039-029AB	...	04 38 12	+28 13 00	12.56	11.31	9.70	Rie14	7.33	5.23	V	14.8	2000.88-2005.06	4.18	13	70	78.61 2.04	Rie14
LP 655-048	...	04 40 23	−05 30 08	17.79	15.72	13.36	Rie14	9.55	8.24	I	12.7	2003.95-2012.89	8.94	21	101	102.61 0.71	Rie14
LHS 1723	...	05 01 57	−06 56 46	12.20	10.86	9.18	Hen06	6.74	5.46	V	19.9	1999.81-2012.75	12.94	35	258	188.66 0.79	Dav14
G 097-015	...	05 04 14	+11 03 23	13.76	12.43	10.74	*	8.31	5.45	R	9.5	2003.95-2010.00	6.04	12	56
LHS 1748	...	05 15 46	−31 17 45	12.08	11.06	9.83	Rie10	7.73	4.35	V	17.1	2000.88-2005.14	4.26	11	58	43.18 1.40	Rie10
GJ 1077	...	05 16 59	−78 17 20	11.90	10.81	9.42	Jao11	7.20	4.70	V	6.6	2003.95-2009.75	5.80	13	64	65.35 1.91	Jao11
L 449-001AB	Y	05 17 22	−35 21 54	11.69	10.48	8.91	Rie14	6.56	5.13	V	24.2	2007.81-2012.96	5.15	17	87	84.38 1.35	Rie14
2MA 0517-3349	...	05 17 37	−33 49 03	19.75	17.38	14.96	Win15	10.83	8.92	I	10.4	2003.95-2012.94	8.99	14	64
LP 717-036	...	05 25 41	−09 09 12	12.59	11.43	9.92	Win15	7.62	4.97	V	15.4	2003.96-2010.17	6.21	12	55
LHS 1767	...	05 31 04	−30 11 44	13.11	11.93	10.45	Rie10	8.19	4.92	V	12.4	2003.96-2007.99	4.03	13	57	65.26 1.51	Rie10
SCR 0533-4257	...	05 33 28	−42 57 20	12.58	11.27	9.59	*	7.12	5.46	R	10.8	2007.81-2012.10	4.29	16	78
WT 178	...	05 37 39	−61 54 43	14.81	13.47	11.77	Rie10	9.23	5.58	R	20.0	1999.92-2012.96	13.04	17	78	62.02 0.89	Rie10
GJ 2045	...	05 42 12	−05 27 55	15.34	13.84	11.93	Jao05	9.37	5.97	I	11.2	2001.15-2013.10	11.96	13	70	79.72 1.89	Jao05
APM 0544-4108	...	05 43 46	−41 08 08	14.12	12.85	11.25	Rie10	8.87	5.25	V	10.4	2000.14-2005.05	4.91	17	76	48.41 0.78	Rie10
G 099-049	...	06 00 03	+02 42 23	11.31	10.04	8.43	Rie14	6.04	5.27	V	15.4	1999.91-2012.94	13.04	56	374	193.60 1.85	Dav14
LHS 1807	...	06 02 22	−20 19 44	13.26	12.10	10.62	Rie10	8.37	4.89	R	7.7	2000.88-2007.83	6.95	12	66	71.00 1.58	Rie10
AP COL	Y	06 04 52	−34 33 36	12.96	11.49	9.60	Rie14	6.87	6.09	V	17.5	2004.74-2011.97	7.22	30	183	119.21 0.98	Rie11
GJ 1088	...	06 10 52	−43 24 17	12.28	11.11	9.61	Rie10	7.31	4.97	V	16.0	2000.88-2005.06	4.18	13	51	87.03 1.28	Rie10
SCR 0613-2742AB	Y	06 13 13	−27 42 06	12.30	11.10	9.55	Rie14	7.15	5.15	V	36.7	2007.82-2013.10	5.29	20	107	34.04 1.00	Rie14
SCR 0630-7643AB	...	06 30 46	−76 43 08	14.82	13.08	11.00	Win11	7.92	6.90	I	7.0	2003.96-2011.97	8.02	22	114	114.16 1.85	Hen06
SCR 0631-8811	...	06 31 31	−88 11 36	15.65	14.05	12.04	Win11	9.07	6.58	I	13.3	2003.94-2013.10	9.16	19	87
L 032-009(A)	...	06 33 43	−75 37 48	10.44	9.37	8.04	Win15	5.86	4.58	V	13.9	2004.00-2010.25	6.22	29	122
L 032-008(B)	...	06 33 46	−75 37 29	11.44	10.29	8.82	*	6.57	4.87	V	15.4	2004.00-2010.25	6.22	27	122
SCR 0640-0552	...	06 40 13	−05 52 23	10.22	9.22	8.03	Win11	5.96	4.26	V	12.3	2004.91-2011.77	6.86	18	107
SCR 0702-6102	...	07 02 50	−61 02 47	16.62	14.75	12.49	Win11	9.52	7.10	I	8.4	2004.00-2011.25	7.40	42	138
SCR 0717-0501	...	07 17 17	−05 01 03	13.29	12.02	10.39	Win11	8.05	5.24	I	11.4	2004.18-2013.11	8.93	19	90
LTT 17957	...	07 17 29	+19 34 16	12.83	11.72	10.35	*	8.16	4.67	R	7.7	2003.94-2009.02	5.08	15	73
L 136-037	...	07 20 52	−62 10 11	12.33	11.18	9.74	Win15	7.52	4.81	I	9.8	2009.09-2012.89	3.81	12	58
SCR 0723-8015AB	...	07 23 59	−80 15 17	17.45	15.61	13.41	Win11	10.44	7.01	I	7.4	2003.07-2013.12	10.05	19	81
G 089-032AB	...	07 36 25	+07 04 43	13.25	11.81	9.97	Hen06	7.28	5.97	R	10.3	1999.91-2005.95	6.05	32	216	116.60 0.97	Hen06
SCR 0740-4257	...	07 40 11	−42 57 40	13.81	12.36	10.50	Win11	7.77	6.04	R	14.6	2004.97-2009.23	4.26	17	99
GJ 283B	...	07 40 21	−17 24 49	16.69	14.69	12.41	Sub09	9.29	7.40	I	8.8	2003.96-2013.95	9.99	24	140	109.79 0.81	Sub09
L 034-026	...	07 49 12	−76 42 06	11.31	10.19	8.79	Rie14	6.58	4.73	V	18.0	2006.21-2012.88	6.68	19	94	94.36 2.11	Rie14
GJ 1103	...	07 51 54	−00 00 12	13.26	11.89	10.19	Win15	7.66	5.60	V	16.4	2003.95-2010.16	6.21	12	77
GJ 300	...	08 12 40	−21 33 06	12.15	10.85	9.22	Hen06	6.71	5.44	V	16.6	1999.91-2012.95	13.05	41	236	122.64 0.49	Dav14
L 098-059	...	08 18 07	−68 18 46	11.71	10.61	9.25	Win15	7.10	4.61	R	9.4	2006.21-2013.26	7.05	18	82

Table 1—Continued

Name	Young	R.A. J2000.0	Dec. J2000.0	V	R	I	Ref.	K_s	$V - K_s$	Filter	Variability (mmag)	Timespan	Duration (yr)	#Nights	#Frames	$\pi_{trig} \pm \sigma$ (mas)	Ref.
(1)	(2)	(3)	(4)	(5)	(6)	(7)	(8)	(9)	(10)	(11)	(12)	(13)	(14)	(15)	(16)	(17)	(18)
LHS 2010	...	08 27 11	-44 59 21	11.86	10.70	9.19	Rie10	6.87	4.99	V	11.2	2001.14-2011.24	10.10	18	110	72.80 1.30	Rie10
LHS 2021	...	08 30 32	+09 47 15	19.21	16.94	14.66	Hen04	10.76	8.45	I	16.3	2003.94-2009.24	5.30	15	54	63.67 1.15	Rie10
GJ 2069ACE	...	08 31 37	+19 23 39	11.93	10.70	9.10	*	6.60	5.33	V	15.5	2004.00-2011.10	7.28	29	79
GJ 2069BD	...	08 31 37	+19 23 39	13.37	12.03	10.30	*	7.72	5.65	V	15.8	2004.00-2011.10	7.28	29	79
SCR 0838-5855	...	08 38 02	-58 55 58	17.19	15.08	12.78	Win11	9.27	7.92	I	8.9	2005.90-2012.96	7.06	16	81
GJ 317	...	08 40 59	-23 27 22	12.01	10.84	9.37	Win15	7.03	4.98	R	17.4	2009.04-2013.38	4.35	15	75	65.54 1.53	Lur14
LHS 2065	...	08 53 36	-03 29 32	18.94	16.74	14.44	Die14	9.94	9.00	I	12.1	2003.95-2013.26	9.31	18	101	117.98 0.76	Die14
LHS 2071AB	...	08 55 20	-23 52 15	13.88	12.55	10.82	Rie10	8.20	5.68	R	16.2	2000.00-2011.50	11.16	30	85	62.84 1.43	Rie10
G 041-014ABC	...	08 58 56	+08 28 26	10.92	9.67	8.05	Hen06	5.69	5.23	V	13.1	1999.97-2011.96	11.98	29	203	147.66 1.98	Hen06
LHS 2090	...	09 00 23	+21 50 04	16.11	14.12	11.84	*	8.44	7.67	I	9.0	2002.28-2010.01	7.73	22	116	156.87 2.67	Hen06
LHS 2106	...	09 07 02	-22 08 50	14.21	12.87	11.13	Rie10	8.65	5.56	R	13.9	2000.06-2006.04	5.97	12	56	66.23 1.16	Rie10
LHS 6167AB	...	09 15 36	-10 35 47	13.82	12.32	10.42	Win15	7.73	6.09	V	32.2	2003.94-2013.25	9.31	23	113
LHS 2122	...	09 16 25	-62 04 16	12.57	11.43	9.94	Rie10	7.55	5.02	R	13.7	2001.15-2009.04	7.89	11	64	58.59 2.57	Rie10
GJ 1123	...	09 17 05	-77 49 23	13.16	11.86	10.16	Jao05	7.45	5.71	V	21.1	2000.00-2010.00	9.78	29	121	110.92 2.02	Jao05
SIP 0921-2104	...	09 21 14	-21 04 44	20.85	18.50	16.17	Win15	11.69	9.16	I	13.5	2004.18-2013.12	8.94	18	66
GJ 357	...	09 36 01	-21 39 38	10.92	9.86	8.57	Win15	6.48	4.44	V	14.5	2004.99-2010.16	5.17	12	96
GJ 358	...	09 39 46	-41 04 03	10.78	9.66	8.27	Win15	6.06	4.72	V	31.7	2004.99-2010.17	5.18	12	75
GJ 1128	...	09 42 46	-68 53 06	12.74	11.39	9.65	Jao05	7.04	5.70	V	14.5	2000.15-2010.00	9.92	33	142	154.27 0.76	Lur14
LHS 5156	...	09 42 49	-63 37 56	13.30	11.98	10.28	Rie10	7.77	5.53	V	9.4	2005.97-2012.96	7.00	15	70	95.15 1.17	Rie10
WT 244	...	09 44 23	-73 58 38	15.17	13.80	12.02	Rie10	9.38	5.79	I	10.4	1999.92-2008.00	8.08	14	64	43.30 1.50	Rie10
GJ 367	...	09 44 29	-45 46 35	10.12	9.10	7.86	Win15	5.78	4.34	V	12.0	2004.99-2010.15	5.16	11	75
G 161-071	...	09 44 54	-12 20 54	13.76	12.26	10.36	Win15	7.60	6.16	V	35.8	2003.94-2012.96	9.02	16	80
LHS 2206	...	09 53 55	+20 56 46	14.02	12.63	10.85	Hen06	8.33	5.69	R	19.1	2000.06-2010.15	10.09	24	145	108.39 2.30	Hen06
LHS 281	...	10 14 51	-47 09 24	13.49	12.26	10.69	Jao05	8.32	5.17	R	15.5	2001.14-2013.27	12.13	15	79	83.07 1.69	Jao05
LP 790-002B	...	10 18 12	-20 28 21	15.56	14.16	12.40	*	9.71	5.85	I	10.6	2005.09-2012.19	7.10	21	97
LP 790-002A	...	10 18 13	-20 28 41	13.95	12.58	10.81	Win15	8.15	5.80	I	12.8	2005.09-2012.19	7.10	21	97
LTT 03790A	...	10 19 51	-41 48 46	11.64	10.66	9.52	Win15	7.49	4.15	V	9.3	2001.27-2005.10	3.91	14	62
LTT 03790B	...	10 19 53	-41 49 01	13.17	12.00	10.49	*	8.29	4.88	V	6.9	2001.27-2005.10	3.91	14	62
LEHPM 2-2758	...	10 38 47	-86 32 44	13.24	12.02	10.46	Win15	8.11	5.13	R	9.5	2006.22-2011.16	4.94	15	67
WT 1827AB	...	10 43 02	-09 12 40	15.11	13.57	11.59	Jao05	8.73	6.38	V	14.7	2000.00-2011.25	11.18	39	92	80.99 2.42	Jao05
LHS 288	...	10 44 21	-61 12 35	13.90	12.31	10.27	Hen06	7.73	6.17	R	9.8	2000.06-2007.39	7.32	20	137	208.95 2.73	Hen06
LHS 292	...	10 48 12	-11 20 09	15.78	13.63	11.25	Die14	7.93	7.85	R	9.4	2000.23-2010.01	9.77	15	76
DEN 1048-3956	...	10 48 14	-39 56 07	17.37	14.98	12.47	Jao05	8.45	8.92	I	10.5	2001.15-2013.27	12.13	33	200	248.08 0.61	Lur14
LHS 2328	...	10 55 34	-09 21 25	13.55	12.37	10.86	Rie10	8.61	4.94	R	17.3	2001.15-2009.25	8.10	14	66	53.84 1.47	Rie10
GJ 406	...	10 56 28	+07 00 53	13.58	11.64	9.44	*	6.08	7.50	R	17.9	2000.23-2012.27	12.04	49	139	415.16 1.62	Dav14
LP 731-076	...	10 58 27	-10 46 30	14.44	13.05	11.24	*	8.64	5.80	I	34.8	2004.43-2011.50	7.07	22	167
LHS 2397aAB	...	11 21 49	-13 13 08	19.43	17.33	14.84	Die14	10.74	8.69	I	23.8	2005.09-2013.26	8.16	22	68	65.83 2.02	Die14
LHS 2401	...	11 23 57	-18 21 48	13.10	11.97	10.54	Rie10	8.32	4.78	V	13.5	2001.15-2009.32	8.17	13	76	54.47 2.51	Rie10
LHS 306	...	11 31 08	-14 57 21	14.19	12.81	11.05	Jao05	8.50	5.69	R	10.1	2001.14-2013.26	12.11	12	74	89.24 1.69	Jao05
TWA 8A	Y	11 32 41	-26 51 55	12.23	11.14	9.79	Rie14	7.43	4.80	V	78.6	2000.14-2011.16	11.02	11	65	21.33 1.41	Rie14
TWA 8B	Y	11 32 41	-26 52 09	15.22	13.68	11.76	Rie14	9.01	6.21	V	124.1	2000.14-2011.16	11.02	11	65	21.22 1.44	Rie14
SCR 1138-7721	...	11 38 16	-77 21 48	14.78	13.20	11.24	Win11	8.52	6.26	I	7.9	2003.00-2010.00	6.91	28	115	120.41 1.01	Lur14
GJ 1147	...	11 38 24	-41 22 32	13.72	12.49	10.91	Rie10	8.54	5.18	R	14.4	2001.15-2009.04	7.89	14	64	66.08 1.08	Rie10
SIP 1141-3624	...	11 41 21	-36 24 34	13.10	11.79	10.10	Win15	7.70	5.40	R	17.5	2007.31-2013.11	5.79	17	84
GJ 438	...	11 43 19	-51 50 25	10.35	9.36	8.27	Rie10	6.32	4.03	V	7.9	2000.06-2009.32	9.26	14	92	91.70 2.05	Rie10
CE 440-087	...	11 47 50	-28 49 44	16.21	14.98	13.38	Win15	11.24	4.97	I	14.1	2001.14-2005.40	4.26	10	50
LP 851-346	...	11 55 42	-22 24 58	18.18	15.97	13.50	Die14	9.88	8.30	I	10.4	2007.18-2013.28	6.10	12	56	89.54 1.77	Die14
SCR 1157-0149	...	11 57 45	-01 49 02	15.99	14.54	12.68	Win11	10.02	5.97	I	11.3	2004.18-2011.11	6.93	13	65

Table 1—Continued

Name	Young	R.A. J2000.0	Dec. J2000.0	V	R	I	Ref.	K_s	$V - K_s$	Filter	Variability (mmag)	Timespan	Duration (yr)	#Nights	#Frames	$\pi_{trig} \pm \sigma$ (mas)	Ref.
(1)	(2)	(3)	(4)	(5)	(6)	(7)	(8)	(9)	(10)	(11)	(12)	(13)	(14)	(15)	(16)	(17)	(18)
RXJ 1159-5247	...	11 59 27	−52 47 19	19.14	16.92	14.49	Win15	10.32	8.82	I	11.4	2009.32-2013.39	4.07	12	59
LHS 2520	...	12 10 05	−15 04 16	12.09	10.88	9.30	Rie10	6.86	5.23	V	10.8	2000.07-2004.43	4.91	10	56	77.93 2.41	Rie10
NLTT 30359	...	12 20 33	−82 25 57	11.96	10.76	9.20	Win15	6.84	5.12	V	11.4	2006.21-2012.26	6.06	22	104
GJ 1157	...	12 23 01	−46 37 08	13.59	12.35	10.71	Rie10	8.36	5.23	V	12.0	2001.14-2011.23	10.09	18	91	62.42 0.63	Rie10
GJ 469AB	...	12 28 57	+08 25 31	12.05	10.85	9.30	*	6.96	5.09	V	16.4	2002.25-2011.00	9.01	22	111
GJ 1158	...	12 29 34	−55 59 37	13.26	12.02	10.41	Jao11	8.07	5.19	V	13.6	2001.15-2008.21	7.06	15	76	76.18 1.38	Jao11
LHS 2568(B)	...	12 29 54	−05 27 20	14.21	12.96	11.37	*	8.92	5.29	R	9.5	2000.07-2009.03	8.96	12	58	48.55 1.81	Rie10
LHS 2567(A)	...	12 29 54	−05 27 24	13.08	11.87	10.33	Rie10	7.96	5.12	R	12.8	2000.07-2009.03	8.96	12	58	46.80 1.83	Rie10
SCR 1230-3411AB	...	12 30 01	−34 11 24	14.16	12.81	11.07	Win11	8.44	5.72	R	8.0	2008.07-2012.53	4.45	10	52
GJ 473AB	...	12 33 17	+09 01 15	12.47	10.90	8.92	*	6.04	6.43	V	15.0	2002.50-2011.00	8.85	26	100
GJ 479	...	12 37 52	−52 00 05	10.66	9.57	8.21	Win15	6.02	4.64	V	9.9	2005.10-2010.50	5.40	19	69
LHS 337	...	12 38 49	−38 22 53	12.75	11.44	9.74	Hen06	7.39	5.36	R	9.0	2002.28-2010.39	8.10	14	105	156.78 1.99	Hen06
SCR 1245-5506	...	12 45 52	−55 06 50	13.66	12.32	10.61	Win11	8.12	5.54	I	9.0	2004.17-2009.08	4.91	12	55
DEN 1250-2121	...	12 50 52	−21 21 13	18.36	16.15	13.78	Die14	10.13	8.23	I	7.8	2005.14-2011.16	6.03	13	45	57.77 1.72	Die14
SIP 1259-4336	...	12 59 04	−43 36 24	18.01	15.74	13.29	Win15	9.52	8.49	I	9.3	2005.06-2013.10	8.04	25	155
WT 1962AB	...	12 59 51	−07 30 35	15.42	14.23	12.68	Win15	10.43	4.99	I	11.0	2000.25-2011.50	11.37	21	91
WT 392	...	13 13 09	−41 30 39	12.90	11.60	9.95	Jao05	7.41	5.49	V	13.7	2000.07-2013.38	13.32	15	72	83.58 1.58	Jao05
LHS 2698	...	13 13 29	−32 27 05	14.21	13.14	11.76	Rie10	9.70	4.51	R	9.5	2000.14-2009.32	9.18	16	69	21.59 0.92	Rie10
LHS 2718	...	13 20 03	−35 24 44	12.84	11.70	10.24	Rie10	7.98	4.86	V	10.7	2001.15-2005.41	4.26	13	70	73.04 0.79	Rie10
LHS 2729	...	13 23 38	−25 54 45	12.89	11.68	10.14	Rie10	7.78	5.11	R	12.3	2001.15-2005.09	3.94	9	56	71.48 1.53	Rie10
G 165-008AB	Y	13 31 46	+29 16 36	12.02	10.77	9.15	Rie14	6.72	5.30	R	17.6	2000.14-2009.25	9.11	31	181	55.51 2.38	Rie14
LHS 2783	...	13 42 09	−16 00 23	13.42	12.14	10.52	Win15	8.09	5.33	R	16.7	2005.09-2011.42	6.32	22	105
LP 739-002	...	13 58 16	−12 02 59	14.46	13.10	11.39	Win15	8.89	5.57	I	10.6	2005.10-2010.16	5.06	15	70
LHS 2836	...	13 59 10	−19 50 03	12.88	11.60	9.90	Rie10	7.45	5.43	V	12.4	2000.14-2012.41	12.28	24	124	92.86 0.89	Rie10
WT 460AB	...	14 11 59	−41 32 21	15.65	13.91	11.80	Hen06	8.62	7.03	I	19.3	2000.14-2012.58	12.44	45	257	107.41 1.52	Hen06
GJ 540.2	...	14 13 04	−12 01 26	13.89	12.52	10.79	Rie14	8.16	5.73	R	14.3	2004.58-2009.49	4.91	15	82
LHS 2899	...	14 21 15	−01 07 19	13.12	11.92	10.39	Rie10	8.09	5.03	V	15.5	2000.14-2005.20	4.99	12	45	74.66 2.15	Rie10
PROXIMA CEN	...	14 29 43	−62 40 46	11.13	9.45	7.41	Jao05	4.38	6.75	V	28.5	2000.57-2013.25	12.68	35	205	768.13 1.04	Lur14
LHS 2935	...	14 32 08	+08 11 31	15.68	14.08	12.09	*	9.17	6.51	R	14.3	2000.14-2009.32	9.19	19	74
GJ 555	...	14 34 16	−12 31 10	11.34	10.06	8.44	Jao05	5.94	5.40	V	13.8	2000.14-2012.26	12.12	32	193	161.73 1.47	Dav14
LHS 3002(B)	...	14 56 27	+17 55 08	18.68	16.65	14.42	*	10.92	7.76	I	10.9	2001.80-2009.50	8.67	17	78	55.64 1.35	Rie10
LHS 3001(A)	...	14 56 27	+17 57 00	15.81	14.35	12.52	Rie10	9.85	5.96	I	11.4	2001.80-2009.50	8.67	17	78	57.17 1.34	Rie10
LHS 3003	...	14 56 38	−28 09 48	16.95	14.90	12.53	Die14	8.93	8.02	I	11.0	2003.52-2010.59	7.07	25	159
2MA 1507-2000	...	15 07 27	−20 00 43	18.82	16.70	14.29	*	10.66	8.16	I	9.7	2004.45-2011.16	6.71	17	74
GJ 581	...	15 19 26	−07 43 20	10.56	9.44	8.03	Win15	5.84	4.72	V	13.2	2000.58-2013.38	12.80	40	267	158.79 1.58	Lur14
LHS 3080AB	...	15 31 54	+28 51 09	14.32	13.01	11.32	Rie10	8.82	5.50	R	11.1	2000.60-2011.50	10.93	25	105	35.52 1.85	Rie10
2MA 1534-1418	...	15 34 56	−14 18 49	19.15	16.71	14.16	Win15	10.31	8.84	I	8.1	2004.60-2012.17	7.57	15	62
GJ 595	...	15 42 06	−19 28 18	11.84	10.73	9.29	Win15	7.17	4.67	V	8.3	2003.51-2010.16	6.65	16	119
L 408-123	...	15 45 41	−43 30 29	13.06	11.90	10.40	Win15	8.08	4.98	R	8.6	2001.60-2011.40	10.85	31	122
LHS 3124	...	15 51 21	+29 31 06	13.03	11.87	10.39	*	8.15	4.88	V	6.4	2001.43-2009.32	7.89	16	67
LHS 5303	...	15 52 44	−26 23 13	16.53	14.66	12.49	Die14	9.32	7.21	I	10.7	2004.57-2012.59	8.02	19	85	94.63 0.70	Die14
LHS 3147	...	16 02 23	−25 05 57	13.20	12.09	10.63	Rie10	8.41	4.79	R	11.8	2001.21-2009.31	8.10	18	72	39.18 1.37	Rie10
LHS 3167	...	16 13 05	−70 09 08	13.71	12.45	10.82	Rie10	8.39	5.32	R	15.0	2000.57-2013.39	12.82	18	96	60.25 0.95	Rie10
LHS 3169	...	16 14 21	−28 30 36	12.95	11.80	10.29	Rie10	8.11	4.84	V	12.0	2000.58-2010.20	9.62	14	67	53.43 1.46	Rie10
GJ 628	...	16 30 18	−12 39 45	10.07	8.89	7.37	Win15	5.08	4.99	V	16.6	2003.51-2012.58	9.07	23	141	230.53 2.24	Dav14
GJ 633	...	16 40 45	−45 59 59	12.67	11.56	10.20	Rie10	8.05	4.62	V	10.7	1999.64-2007.44	7.79	20	100	59.47 1.19	Rie10
GJ 2122AB	...	16 45 16	−38 48 33	9.68	8.73	7.69	*	5.72	3.96	V	12.2	2000.58-2012.25	11.68	31	164
G 169-029	...	16 50 57	+22 27 05	14.08	12.69	10.91	*	8.31	5.77	R	14.6	2000.57-2009.57	9.00	25	120

Table 1—Continued

Name	Young	R.A. J2000.0	Dec. J2000.0	V	R	I	Ref.	K_s	$V - K_s$	Filter	Variability (mmag)	Timespan	Duration (yr)	#Nights	#Frames	$\pi_{trig} \pm \sigma$ (mas)	Ref.
(1)	(2)	(3)	(4)	(5)	(6)	(7)	(8)	(9)	(10)	(11)	(12)	(13)	(14)	(15)	(16)	(17)	(18)
GJ 643	...	16 55 25	−08 19 21	11.77	10.55	9.01	*	6.72	5.05	V	9.0	2003.52-2011.55	8.03	18	113
GJ 1207	...	16 57 05	−04 20 56	12.25	11.00	9.43	Hen06	7.12	5.13	V	196.3	1999.62-2012.58	12.95	43	232	115.39 1.51	Hen06
GJ 1215AB	...	17 17 44	+11 40 11	15.07	13.57	11.68	*	8.93	6.14	I	11.0	2002.46-2012.28	9.82	36	196
GJ 667C	...	17 18 58	−34 59 48	10.34	9.29	8.09	*	6.04	4.30	V	10.6	2003.52-2013.38	9.86	23	140	140.88 2.04	Lur14
GJ 682	...	17 37 03	−44 19 09	10.99	9.75	8.15	Win15	5.61	5.38	V	12.9	2003.52-2009.24	5.72	18	158
GJ 693	...	17 46 34	−57 19 08	10.77	9.62	8.20	Win15	6.02	4.75	V	11.9	2003.51-2009.62	6.11	18	138
GJ 1224	...	18 07 32	−15 57 47	13.48	12.08	10.31	Rie14	7.83	5.65	I	12.7	2003.52-2012.52	9.00	25	170	126.54 1.05	Rie14
SCR 1826-6542	...	18 26 46	−65 42 39	17.35	15.28	12.96	Win11	9.55	7.80	I	9.4	2005.71-2013.67	7.96	17	79
G 141-021	...	18 36 19	+13 36 26	12.45	11.23	9.69	*	7.37	5.08	R	11.6	2003.52-2007.54	4.02	14	78
SCR 1841-4347	...	18 41 09	−43 47 32	16.46	14.72	12.59	Win11	9.60	6.86	I	11.3	2007.55-2013.38	5.83	13	61
G 141-029	...	18 42 44	+13 54 17	12.86	11.58	9.95	Rie14	7.55	5.31	I	12.7	2003.52-2012.58	9.06	17	82	90.09 1.91	Rie14
LHS 5341	...	18 43 06	−54 36 48	12.97	11.68	10.03	Win15	7.49	5.48	R	15.5	2006.79-2012.69	5.91	18	90
SCR 1845-6357AB	...	18 45 05	−63 57 47	17.40	15.00	12.46	Win11	8.51	8.89	I	8.9	2003.00-2011.50	8.30	63	220	259.45 1.11	Hen06
SCR 1848-6855AB	...	18 48 21	−68 55 34	16.86	15.68	13.83	Jao14	11.10	5.76	I	8.9	2003.24-2012.58	9.34	33	151	40.63 0.72	Jao14
GJ 729	...	18 49 49	−23 50 10	10.50	9.26	7.68	Win15	5.37	5.13	V	11.1	1999.62-2012.75	13.13	19	124	339.59 1.63	Dav14
SCR 1855-6914	...	18 55 47	−69 14 15	16.61	14.79	12.66	Win11	9.51	7.10	I	7.4	2003.51-2013.66	10.15	16	82
GJ 748AB	...	19 12 14	+02 53 11	11.10	9.95	8.47	Win15	6.29	4.81	V	9.4	2004.50-2011.75	7.29	33	141	99.99 1.22	Lur14
LHS 3443	...	19 13 07	−39 01 53	12.39	11.27	9.85	Rie10	7.66	4.73	V	9.4	2000.58-2009.75	9.17	14	69	48.57 1.14	Rie10
LHS 475	...	19 20 54	−82 33 16	12.69	11.51	10.00	Jao11	7.69	5.00	V	11.0	2000.57-2009.55	8.97	26	132	83.04 0.93	Jao11
SCR 1931-0306	...	19 31 04	−03 06 18	16.81	15.11	13.11	Win11	10.23	6.58	I	15.9	2004.58-2010.58	6.00	19	79
LP 869-019	...	19 42 00	−21 04 05	13.22	11.93	10.28	Win15	7.82	5.40	R	13.2	2004.57-2009.31	4.74	13	63
LP 869-026AB	...	19 44 53	−23 37 59	14.09	12.65	10.85	Win15	8.27	5.82	R	11.2	2004.57-2008.71	4.14	14	55
LHS 3484	...	19 47 04	−71 05 33	13.88	12.70	11.19	Rie10	8.98	4.90	R	7.7	2000.58-2009.32	8.75	14	65	39.65 1.52	Rie10
LHS 3492	...	19 51 31	−50 55 37	15.27	14.05	12.45	Win15	10.19	5.08	I	8.3	2007.56-2011.62	4.05	12	60
LP 870-065	...	20 04 30	−23 42 02	13.02	11.75	10.09	Win15	7.70	5.32	R	13.3	2004.57-2010.50	5.92	18	68
2MA 2009-0113	...	20 09 18	−01 13 38	14.47	12.98	11.16	Rie14	8.51	5.96	I	15.2	2004.73-2013.39	8.66	14	71	95.95 1.54	Rie14
SCR 2010-2801AB	Y	20 10 00	−28 01 41	12.98	11.78	10.20	Rie14	7.73	5.25	R	11.1	2007.82-2011.62	3.80	13	63	20.85 1.33	Rie14
LEHPM 2-0783	...	20 19 49	−58 16 43	17.17	15.28	13.03	Rie14	9.72	7.45	I	18.3	2006.37-2013.66	7.29	13	68	61.93 1.02	Rie14
GJ 1251	...	20 28 03	−76 40 15	13.88	12.58	10.91	Jao05	8.60	5.28	R	15.7	1999.62-2013.67	14.05	15	80	79.02 2.25	Jao05
L 755-019	Y	20 28 43	−11 28 30	12.47	11.31	9.81	Rie14	7.50	4.97	R	17.2	2007.82-2012.42	4.60	11	56	53.18 1.67	Rie14
GJ 791.2AB	...	20 29 48	+09 41 20	13.13	11.73	9.97	*	7.31	5.82	I	8.2	2004.50-2011.75	7.40	30	148
LEHPM 2-1265	...	20 33 01	−49 03 10	15.33	13.84	11.98	Win11	9.19	6.14	R	11.7	2008.64-2013.80	5.16	20	89
SCR 2033-2556	Y	20 33 37	−25 56 52	14.87	13.44	11.57	Rie14	8.88	5.99	R	16.4	2008.71-2013.80	5.09	12	53	20.70 1.43	Rie14
SCR 2036-3607	...	20 36 08	−36 07 11	11.66	10.59	9.27	Rie14	7.17	4.49	V	23.4	2007.83-2013.80	5.97	13	69	62.13 1.40	Rie14
LHS 3583	...	20 46 37	−81 43 13	11.50	10.39	9.02	Rie10	6.83	4.67	V	13.4	2000.57-2009.32	8.75	14	68	94.72 2.38	Rie10
LP 756-003	...	20 46 43	−11 48 13	13.80	12.52	10.88	Win15	8.44	5.36	R	18.9	2004.58-2010.73	6.15	15	68
SCR 2049-4012	...	20 49 09	−40 12 06	13.53	12.12	10.31	*	7.70	5.83	R	15.6	2007.82-2012.75	4.93	15	76
LP 816-060	...	20 52 33	−16 58 29	11.50	10.25	8.64	Win15	6.20	5.30	V	15.6	2003.52-2009.62	6.10	14	117
GJ 810AC	...	20 55 37	−14 02 08	12.48	11.23	9.62	Jao11	7.37	5.11	V	14.9	1999.71-2011.65	12.03	33	101	73.08 1.17	Jao11
GJ 810B	...	20 55 37	−14 02 08	14.64	13.21	11.41	*	8.92	5.72	V	14.3	1999.71-2011.65	12.03	32	101	82.79 1.24	Jao11
NLT 50324	...	21 02 24	−60 31 36	11.96	10.97	9.79	Win15	7.71	4.25	V	13.9	2006.37-2011.42	5.06	11	60
APM 2127-3844	...	21 27 04	−38 44 50	14.60	13.31	11.66	Rie10	9.28	5.32	R	15.5	1999.62-2004.73	5.11	12	58	49.25 1.38	Rie10
LHS 510	...	21 30 47	−40 42 29	13.12	11.92	10.35	Jao05	8.13	4.99	R	19.3	2000.57-2013.39	12.82	14	77	83.60 2.52	Jao05
GJ 831AB	...	21 31 18	−09 47 26	12.02	10.70	9.00	Win15	6.38	5.64	V	19.7	2003.50-2012.00	8.21	36	184
WT 795	...	21 36 25	−44 01 00	14.15	12.80	11.08	Rie10	8.53	5.62	V	15.9	2000.41-2004.44	4.03	17	74	69.53 0.70	Rie10
LHS 512	...	21 38 43	−33 39 55	12.55	11.37	9.88	Jao05	7.57	4.98	V	11.9	2000.57-2012.81	12.24	12	72	82.02 2.10	Jao05
LHS 3738(BC)	...	21 58 49	−32 26 25	15.78	14.29	12.46	*	9.76	6.02	R	11.9	1999.64-2012.69	13.05	30	146	52.22 1.03	Lur14
LHS 3739(A)	...	21 58 50	−32 28 17	14.72	13.45	11.88	Rie10	9.56	5.16	R	10.0	1999.64-2012.69	13.05	30	146	50.97 1.05	Rie10

Table 1—Continued

Name	Young	R.A. J2000.0	Dec. J2000.0	V	R	I	Ref.	K_s	$V - K_s$	Filter	Variability (mmag)	Timespan	Duration (yr)	#Nights	#Frames	$\pi_{trig} \pm \sigma$ (mas)	Ref.
(1)	(2)	(3)	(4)	(5)	(6)	(7)	(8)	(9)	(10)	(11)	(12)	(13)	(14)	(15)	(16)	(17)	(18)
WT 870	...	22 06 40	−44 58 07	14.43	13.10	11.40	Rie10	8.89	5.54	R	14.6	2000.41-2005.90	5.48	15	70	56.51 1.13	Rie10
GJ 849	...	22 09 40	−04 38 26	10.38	9.27	7.87	Win15	5.59	4.79	V	11.7	2003.52-2013.39	9.86	21	135	116.05 1.99	Lur14
LHS 3799	...	22 23 07	−17 36 26	13.30	11.87	10.04	Rie14	7.32	5.98	V	13.8	2003.52-2012.70	9.18	21	118	138.17 1.87	Rie14
LEHPM 1-4771	...	22 30 09	−53 44 55	14.47	13.09	11.30	Win15	8.63	5.84	R	17.7	2006.78-2012.69	5.91	14	69
LHS 3836	...	22 38 02	−65 50 08	14.34	13.14	11.61	Rie10	9.41	4.93	R	9.6	1999.62-2004.45	4.82	11	61	36.42 1.32	Rie10
LP 876-010	...	22 48 04	−24 22 07	12.59	11.31	9.61	Mam13	7.21	5.38	V	12.0	2004.44-2012.88	8.44	25	118	132.07 1.19	Mam13
LP 932-083	...	22 49 08	−28 51 20	13.94	12.67	10.98	Win15	8.47	5.47	V	46.4	2004.58-2011.50	6.92	11	47
GJ 876	...	22 53 16	−14 15 49	10.18	8.97	7.40	Win15	5.01	5.17	V	17.2	2003.52-2013.39	9.87	29	85	213.11 4.03	Lur14
GJ 1277	...	22 56 24	−60 03 49	14.00	12.59	10.79	Jao11	8.11	5.89	V	6.8	2001.70-2007.80	5.95	25	80	97.48 1.17	Jao11
SCR 2303-4650	...	23 03 35	−46 50 47	13.89	12.54	10.83	*	8.36	5.53	V	10.0	2009.63-2013.65	4.02	14	68
2MA 2306-0502	...	23 06 29	−05 02 29	18.75	16.54	14.10	Win15	10.30	8.45	I	14.3	2004.58-2009.75	5.17	12	47
SSS 2307-5008	...	23 06 58	−50 08 58	21.36	18.90	16.46	Die14	12.24	9.12	I	11.2	2009.55-2013.80	4.25	14	44	46.59 1.57	Die14
LHS 3925	...	23 17 50	−48 18 47	13.61	12.44	10.92	Rie10	8.71	4.90	R	8.6	2000.58-2005.80	5.23	12	62	46.85 1.17	Rie10
GJ 1284AB	...	23 30 13	−20 23 27	11.14	10.02	8.59	Rie14	6.33	4.81	V	27.1	2003.51-2011.51	8.00	20	95	67.90 2.29	Rie14
GJ 1286	...	23 35 10	−02 23 20	14.73	13.10	11.10	Win15	8.18	6.55	I	13.8	2003.52-2012.88	9.36	23	135	141.47 1.10	Dav14
LHS 547	...	23 36 52	−36 28 51	13.76	12.46	10.79	Jao05	8.42	5.34	V	25.5	2000.57-2012.88	12.31	20	84	86.23 2.03	Jao05
LHS 4009AB	...	23 45 31	−16 10 20	14.38	12.90	10.99	Rie10	8.31	6.07	R	10.6	1999.62-2009.78	10.15	17	83	79.97 1.37	Rie10
LHS 4016AB	...	23 48 36	−27 39 38	12.34	11.25	9.90	Rie14	7.74	4.60	V	14.1	2000.87-2011.74	10.87	21	97	41.25 1.55	Rie10
LHS 4021	...	23 50 31	−09 33 32	13.44	12.19	10.59	Rie10	8.04	5.40	V	17.3	2000.71-2004.89	4.10	15	60	62.41 1.70	Rie10
LEHPM 1-6333AB	...	23 51 50	−25 37 36	19.98	17.86	15.47	Win15	11.27	8.71	I	9.5	2004.58-2012.88	8.30	22	65
L 085-031	...	23 53 25	−70 56 41	13.01	11.78	10.18	Win15	7.78	5.23	I	8.3	2006.53-2013.65	7.12	14	73
LEHPM 1-6494	...	23 56 10	−34 26 04	20.81	18.34	15.89	Die14	11.97	8.84	I	10.6	2009.56-2013.80	4.25	10	29	52.37 1.71	Die14
LTT 09828AB	...	23 59 44	−44 05 00	12.81	11.67	10.23	Win15	8.04	4.77	V	10.4	2000.58-2012.58	12.00	18	89
LHS 4058	...	23 59 51	−34 06 42	12.84	11.64	10.08	Rie10	7.75	5.09	V	9.7	2000.41-2006.87	4.20	16	59	63.14 2.02	Rie10

es: “Y” in Column 2 indicates stars confirmed to be young in Riedel et al. (2014). VRI photometry is from this paper = *, Dieterich et al. (2014) = Die14, y et al. (2004) = Hen04, Henry et al. (2006) = Hen06, Jao et al. (2005) = Jao05, Jao et al. (2011) = Jao11, Jao et al. (2014) = Jao14, Mamajek et al. (2013) am13, Riedel et al. (2010) = Rie10, Riedel et al. (2014) = Rie14, Subasavage et al. (2009) = Sub09, Winters et al. (2011) = Win11, and Winters et al. (2015) = Win15.

Table 2. M Dwarfs Nearer than 25 Parsecs with Exoplanets

Name	# Planets	V	R	I	Ref.	$V - K_s$	Filter	Variability (mmag)	Duration (yr)	# Nights	# Frames
GJ 163	3	11.84	10.76	9.34	Bes90	4.71
GJ 176	1	9.98	8.95	7.72	Wei96	4.37
GJ 179	1	11.98	10.83	9.33	Bes90	5.04
GJ 317	1	12.01	10.84	9.37	Win15	4.98	R	17.4	4.35	15	75
GJ 433	1	9.84	8.84	7.69	Bes90	4.22
GJ 436	1	10.65	9.58	8.25	Wei96	4.58
GJ 581	4	10.56	9.44	8.03	Win15	4.72	V	13.2	12.80	40	267
GJ 649	1	9.69	8.72	7.63	Wei96	4.07
GJ 667 C	2	10.34	9.29	8.09	*	4.30	V	10.6	9.85	23	140
GJ 674	1	9.37	8.28	6.97	Win15	4.52
GJ 832	1	8.66	7.66	6.48	Bes90	4.16
GJ 849	1	10.38	9.27	7.87	Win15	4.79	V	11.7	9.87	21	135
GJ 876	4	10.18	8.97	7.40	Win15	5.17	V	17.2	9.87	29	85
GJ 1148	1	11.92	10.73	9.18	Wei96	5.10
GJ 1214 ^a	1	14.71	13.27	11.50	*	5.93	I	15.6	3.00	15	80
LHS 2335 ^a	1	11.93	10.90	9.63	Rie10	4.46	V	10.3	2.00	9	56
LP 804-027	1	11.37	10.29	8.92	Koe10	4.78

Notes: VRI photometry is from this paper = *, Bessel (1990) = Bes90, Koen et al. (2010) = Koe10, Weis (1996) = Wei96, and our program, Riedel et al. (2010) = Rie10, Winters et al. (2015) = Win15. $V - K_s$ uses K_s from 2MASS. For seven stars, the filter listed is used to observe the star for parallax and photometric variability. The two stars indicated with ^a are being observed but not included in the larger study discussed here because they do not yet have four years of observations. Stars not observed in this program are listed for completeness, with the filter, variability, and coverage metrics left blank.

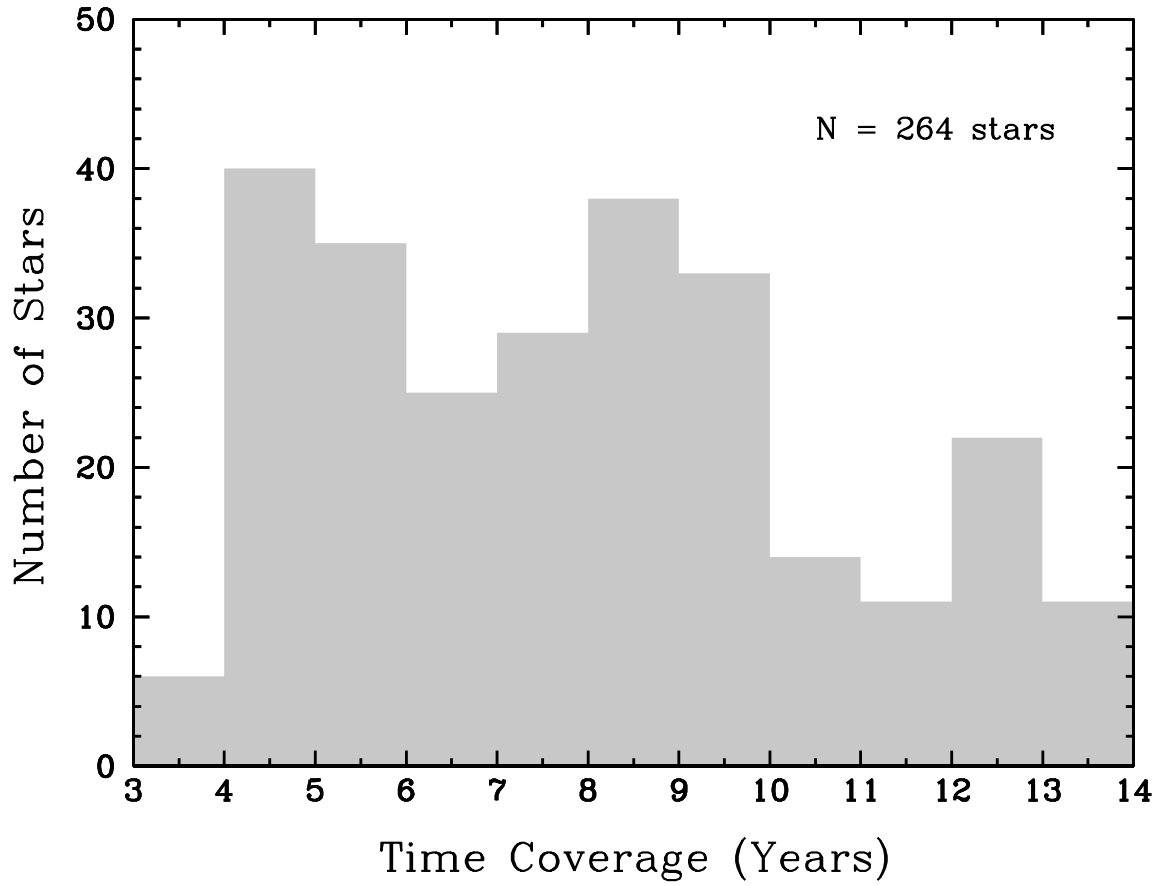


Fig. 1.— This histogram outlines the photometric variability time coverage for the sample stars, listed individually in Table 1. The median time coverage is 7.9 years. Some stars were not observed uniformly throughout the time period, i.e. they had fewer than three nights of observations in some years.

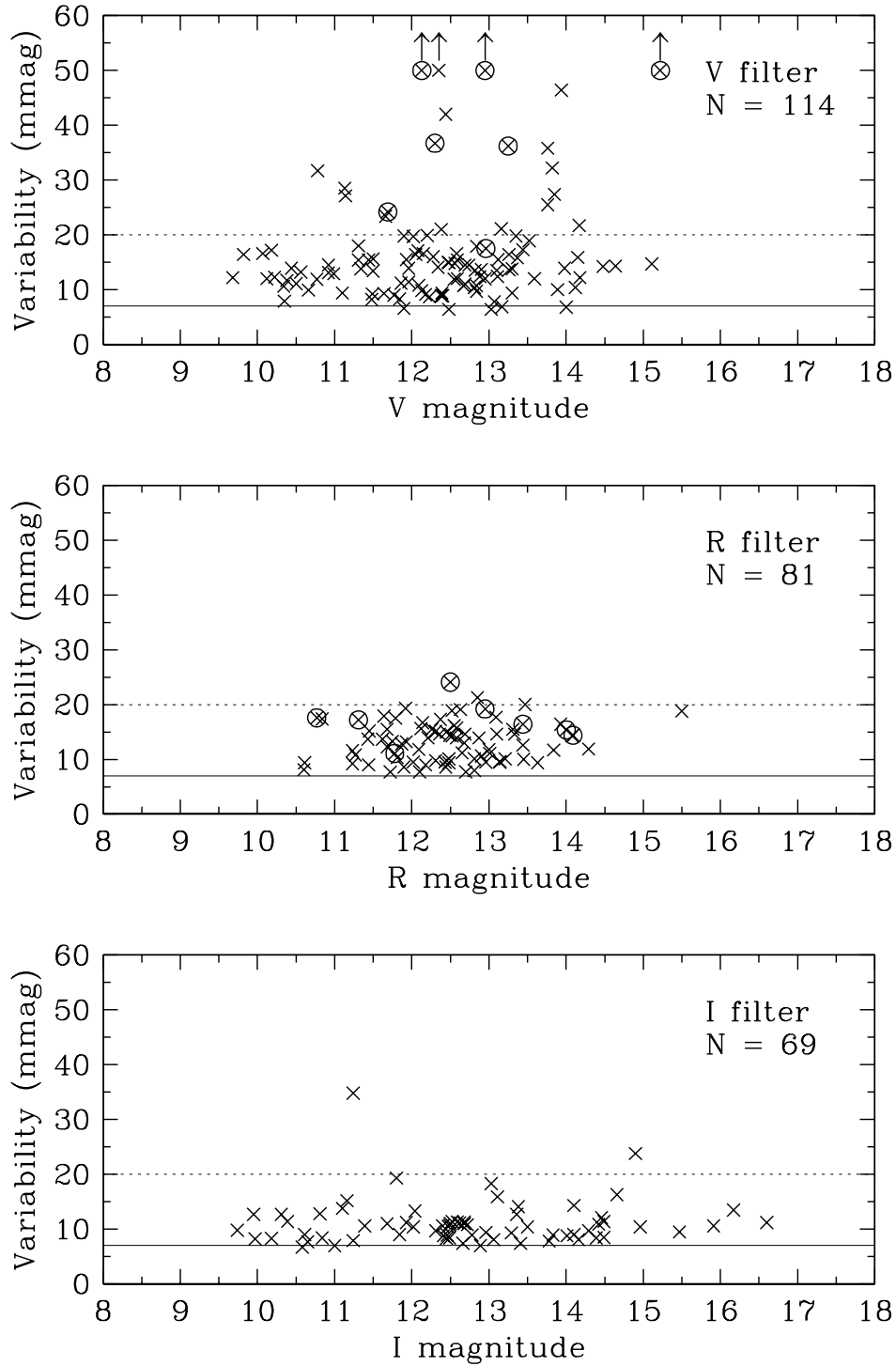


Fig. 2.— The photometric variability defined as the standard deviation of a target star’s brightness relative to reference stars in the field, is shown in each of the three filters used for long-term astrometric measurements, *VRI*, as a function of target brightness. Circled points represent stars denoted as young, with “Y” beside their names in Table 1. Four stars discussed in the text vary by more than 50 mmag at *V* and are represented by arrowed points in the *V* panel. There are no obvious trends in photometric variability with apparent magnitude, with a variability floor represented by solid lines at 7 mmag in all three filters. Dotted lines at 20 mmag indicate our selected threshold between active (above) and quiescent (below) stars.

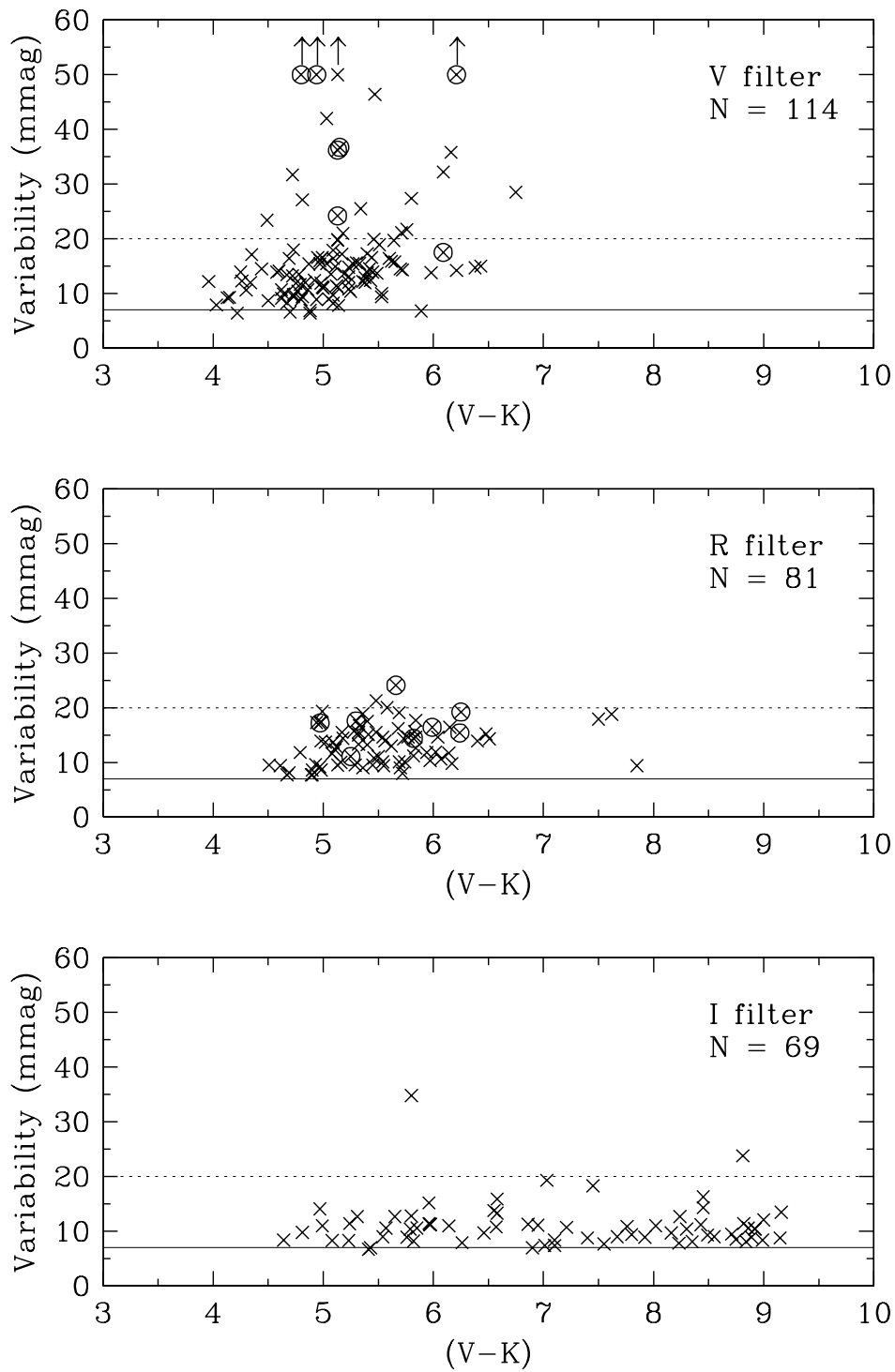


Fig. 3.— The photometric variability is shown in each of the three filters used for long-term astrometric measurements, VRI , as a function of target $V-K$ color. There are no obvious trends in photometric variability with temperature. See the caption of Figure 2 for additional details of the plot format.

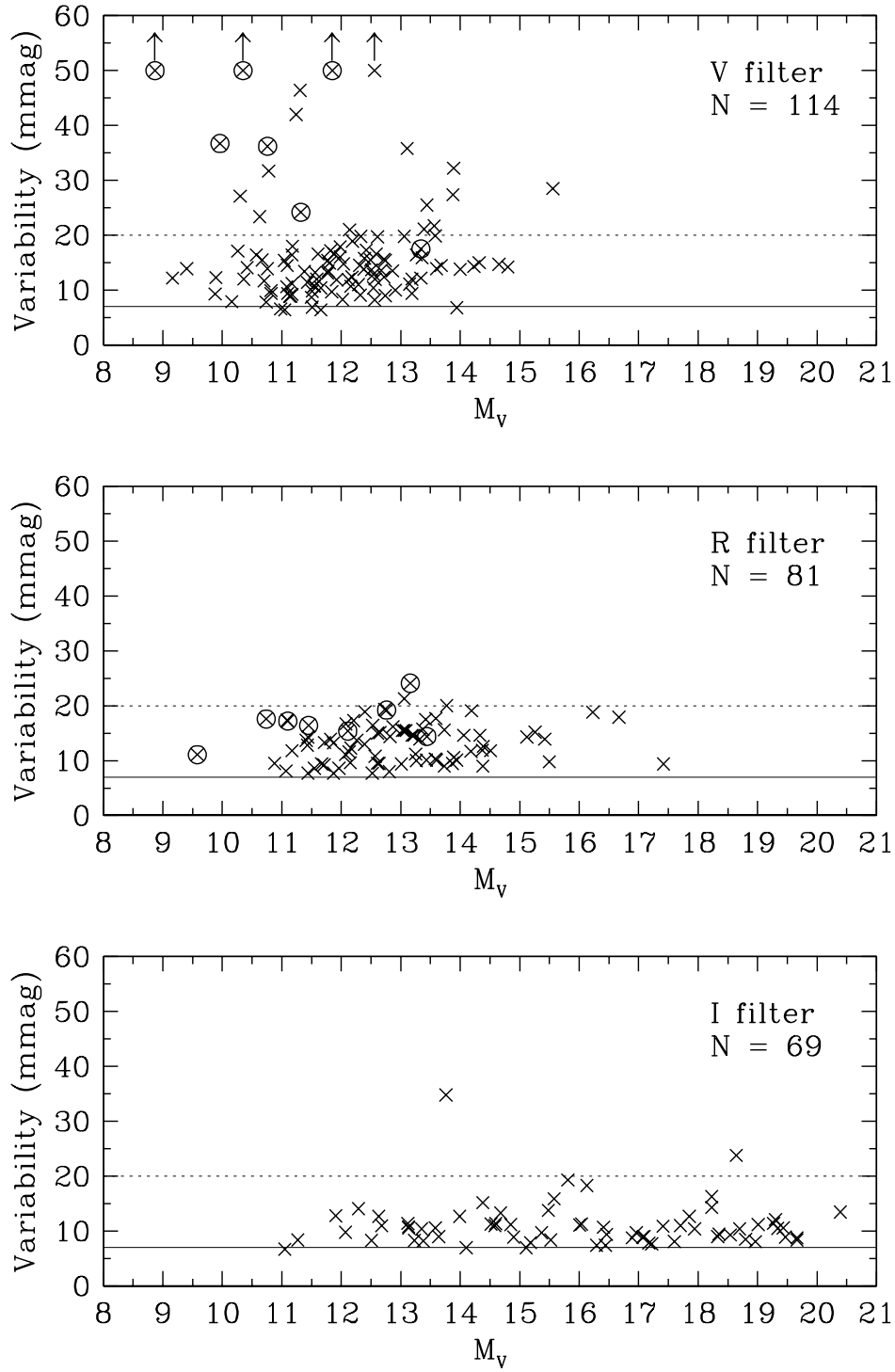


Fig. 4.— The photometric variability is shown in each of the three filters used for long-term astrometric measurements, *VRI*, as a function of absolute magnitude. There are no obvious trends in photometric variability with luminosity. See the caption of Figure 2 for additional details of the plot format.

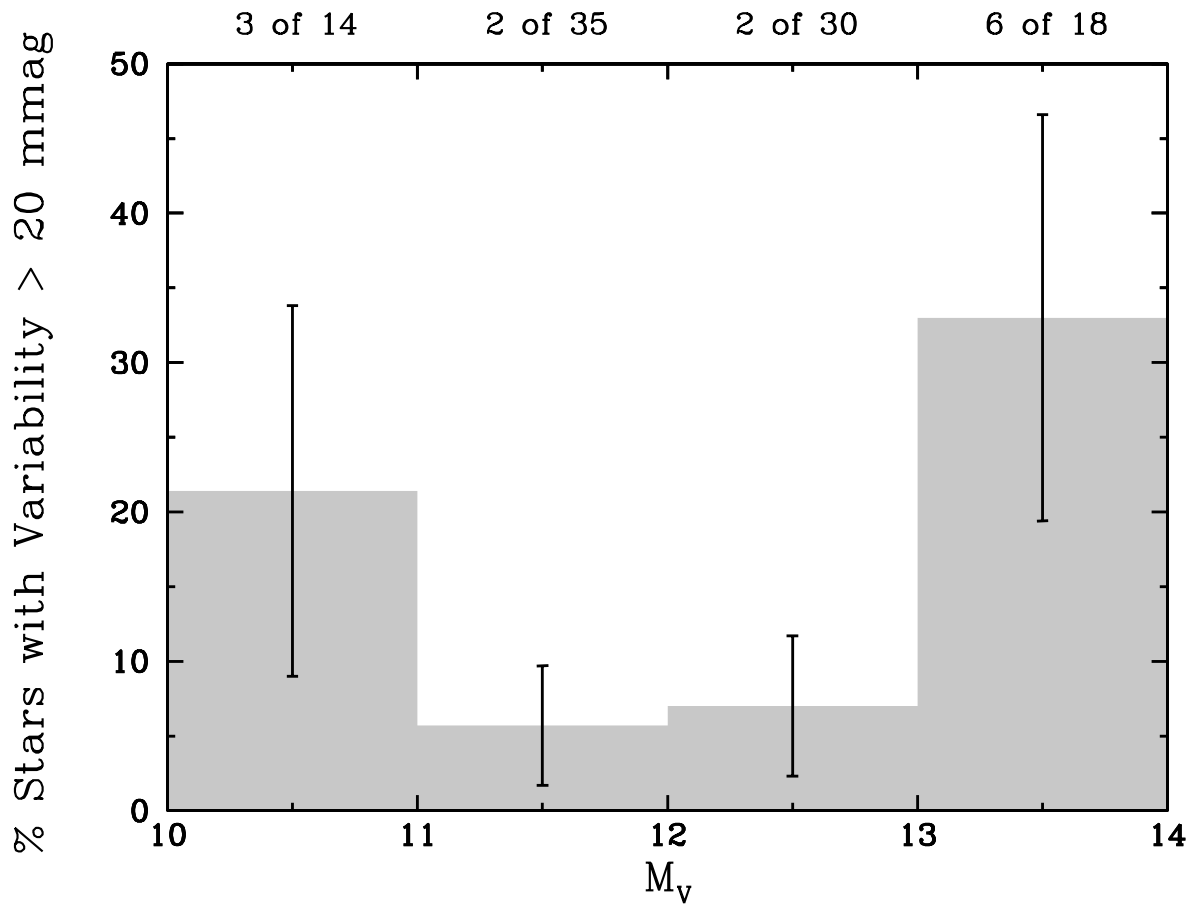


Fig. 5.— The fractions of variable stars within 25 pc observed in the V filter are shown, setting the variability threshold at 20 mmag. In total, there are 106 stars in the sample, of which 14 (13%) vary by more than 20 mmag. Nine stars are not shown because they fall in one brighter bin and two fainter bins with too few stars to be statistically useful. Large error bars represent counting statistics, illustrating that the sample suffers from small numbers of detected variable stars. This precludes detecting any clear trends in variability in the current dataset.

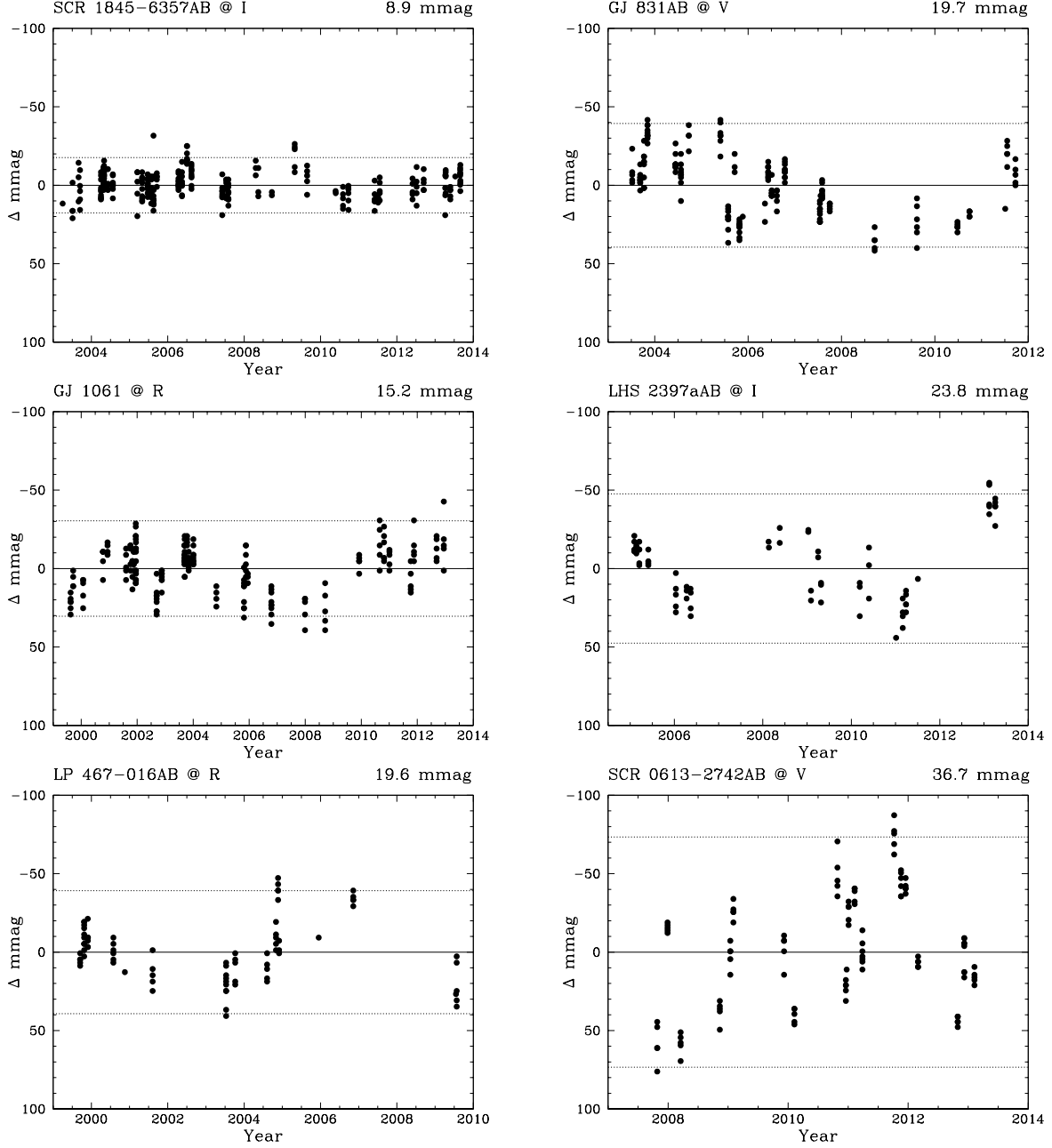


Fig. 6.— Each panel illustrates the brightness for one target measured relative to a set of observed background reference stars, where each point represents an individual image. The filter for the observations is given in the upper left of each panel after the target name. The relative brightnesses are given as magnitude differences, measured in milli-magnitudes, with the average deviation from zero listed at the top right. The star is brighter when points are plotted toward the top, i.e. at negative offsets. Dotted lines represent offsets twice that of the average deviation. The upper left panel for SCR 1845-6357AB shows a non-variable star. The other five panels show stars with periodic variations.

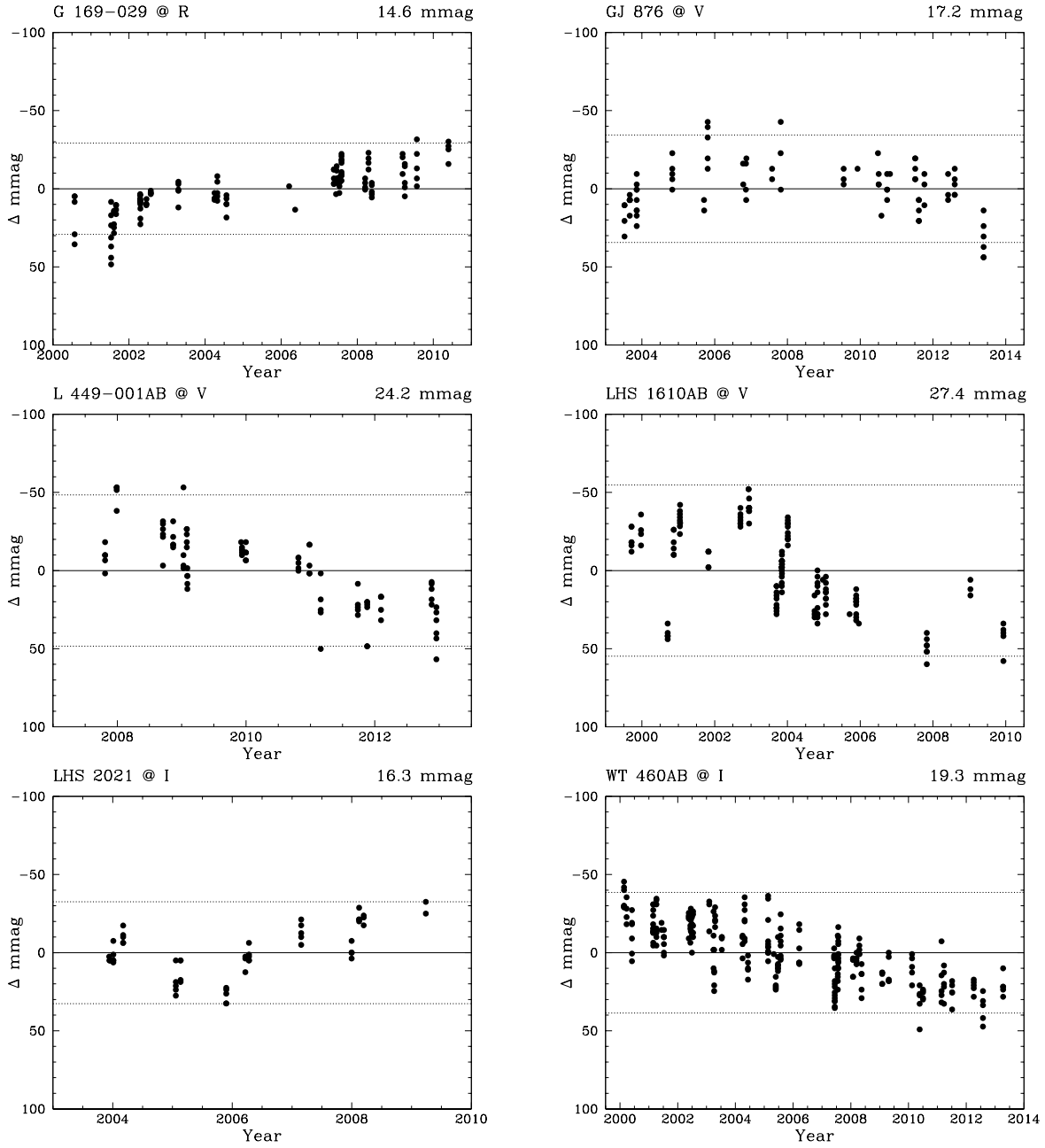


Fig. 7.— See Figure 6 caption for plot layout details. Each of the six stars shown exhibits a long-term trend that does not appear to have yet completed a full cycle in the available datasets.

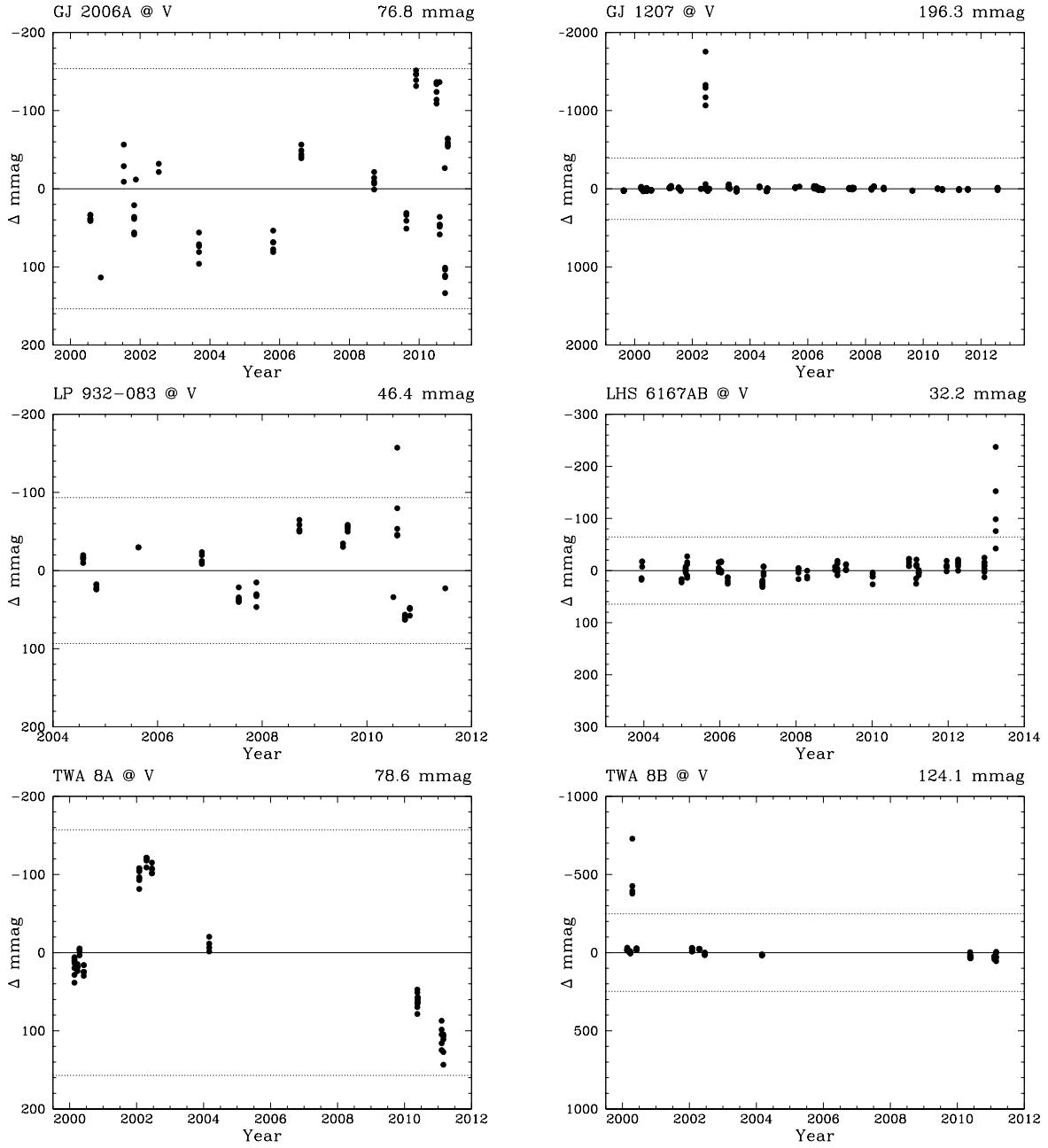


Fig. 8.— See Figure 6 caption for plot layout details. The three left panels show data for stars that appear to show evidence of spots, whereas the three right panels show stars with obvious flare events.